Polarised subcellular activation of ROPs by specific ROPGEFs drives pollen germination in *Arabidopsis thaliana*

Authors:

Alida Melissa Bouatta[1], Andrea Lepper[1], Philipp Denninger [1,*]

[1] Technical University of Munich, School of Life Sciences, Plant Systems Biology,
  Emil-Ramann-Strasse 8, 85354 Freising, Germany

[*] Corresponding author:
  Email: philipp.denninger@tum.de, ORCID ID: https://orcid.org/0000-0003-3794-2360

1 **Abstract**

2 During plant fertilisation, excess male gametes compete for a limited number of female

3 gametes. The dormant male gametophyte, encapsulated in the pollen grain, consists of two

4 sperm cells enclosed in a vegetative cell. After reaching the stigma of a compatible flower,

5 quick and efficient germination of the vegetative cell to a tip-growing pollen tube is crucial to

6 ensure fertilisation success. RHO OF PLANTS (ROP) signalling and their activating ROP

7 GUANINE NUCLEOTIDE EXCHANGE FACTORS (ROPGEFs) are essential for initiating

8 polar growth processes in multiple cell types. However, which ROPGEFs activate pollen

9 germination is unknown. We investigated the role of ROPGEFs in initiating pollen germination

10 and the required cell polarity establishment. Of the five pollen-expressed ROPGEFs, we found

11 that GEF8, GEF9, and GEF12 are required for pollen germination and male fertilisation

12 success, as *gef8;gef9;gef12* triple mutants showed almost complete loss of pollen germination

13 *in vitro* and had a reduced allele transmission rate. Live cell imaging and spatiotemporal

14 analysis of subcellular protein distribution showed that GEF8 and GEF9, but not GEF12,

15 displayed transient polar protein accumulations at the future site of pollen germination minutes

16 before pollen germination, demonstrating specific roles for GEF8 and GEF9 during the

17 initiation of pollen germination. Furthermore, this novel GEF accumulation appears in a

18 biphasic temporal manner and can shift its location. We showed that the C-terminal domain of

19 GEF8 and GEF9 confers this protein accumulation and demonstrated that GEFs locally

20 activate ROPs and alter Ca^{2+} signalling, which is required for pollen tube germination. We

21 demonstrated that GEFs do not act redundantly during pollen germination and described for

22 the first time a polar domain with spatiotemporal flexibility, which is crucial for the *de novo*

23 establishment of a polar growth domain within a cell and, thus, for pollen function and

24 fertilisation success.

Introduction

25

26 Sexual reproduction is a fundamental and complex process in which male and female gametes

27 fuse to form a zygote, which develops into an embryo. In Angiosperms, sperm cells have lost

28 their motility, and the male gametes must be delivered to the female gametes. This is achieved

29 by a tip-growing pollen tube formed by the vegetative pollen cell, which encloses two sperm

30 cells. This pollen tube grows from the papilla cells of the stigma on the flower surface into the

31 transmitting tract toward the female gametophyte inside the ovary. After reaching the female

32 gametophyte, the pollen tube ruptures and releases its enclosed sperm cells. In the last step

33 of double fertilisation, which is characterised by defined Ca^{2+} signals in the female gametes,

34 the sperm cells subsequently fuse with the egg cell and the central cell to form the zygote and

35 the endosperm, respectively (Dresselhaus and Franklin-Tong, 2013; Bleckmann et al., 2014;

36 Denninger et al., 2014; Hamamura et al., 2014; Sprunck, 2020).

37 To protect the male gametophyte from environmental influences on its way to a compatible

38 flower, it is metabolically inactive, desiccated, and encapsulated in a thick and rigid pollen

39 coat, forming the pollen grain. Once on the stigma of a compatible flower, the vegetative cell

40 needs to be activated and polarise the tip growth machinery to a defined subcellular region to

41 germinate from the pollen grain (Edlund et al., 2004; Rudall and Bateman, 2007). Pollen grains

42 have apertures, areas in which the pollen coat is thinner, which predefine the possible

43 emergence regions of the pollen tube in most angiosperms. However, in some species, such

44 as *Arabidopsis thaliana,* the pollen emergence site is independent of these apertures and is

45 predominantly defined by the contact site to the papilla cells. This requires sensing the contact

46 site and a growth machinery, which can be polarised independently of the pollen morphology

47 to loosen the pollen coat locally and allow the pollen tube's subsequent polar emergence

48 (Edlund et al., 2004). Moreover, in most Angiosperms, the number of pollen grains exceeds

49 the number of female gametes, causing competition between the individual pollen grains.

50 Thus, the rapid establishment of cell polarity and polar growth initiation required for pollen

51 germination is crucial in this competition and is decisive for fertilisation success. (Dresselhaus

52 et al., 2016; Sprunck, 2020). The factors responsible for sensing the papilla-pollen contact site

53 and the polarisation of the tip growth machinery in pollen grains are unknown. Moreover, the

54 proteins required to transmit this polarisation signal to the tip growth machinery have yet to be

55 discovered. Therefore, we investigated this crucial aspect of pollen germination.

56 During pollen tube tip growth, multiple RECEPTOR-LIKE KINASES (RLKs), like POLLEN

57 RECEPTOR KINASEs (PRKs), BUDDHA'S PAPER SEAL (BUPS), or ANXUR (ANX) RLKs

58 were shown to be required for pollen tube growth. BUPS and ANX RLKs are crucial for

59 maintaining pollen tube integrity and preventing the rupture of germinated pollen tubes

60 (Boisson-Dernier et al., 2009; Miyazaki et al., 2009; Ge et al., 2017). PRKs promote general

61 pollen tube growth and are required for chemotaxis towards the female gametophyte (Mu et

62   al., 1994; Tang et al., 2004; Chang et al., 2013; Takeuchi and Higashiyama, 2016). PRKs
63   were also proposed to sense stigmatic signal peptides in Tomato and thus activate pollen
64   germination, but no general germination-promoting function for these RLKs is shown
65   (Muschietti et al., 1998; Tang et al., 2004; Chang et al., 2013). Thus, it is still unknown whether
66   PRKs play a general role in pollen activation and germination or which proteins are crucial for
67   initiating pollen activation.

68   In various cell types and processes, RLKs activate RHO OF PLANTS (ROP) signalling
69   pathways to establish cell polarity, promote polar growth, or confer immune responses
70   (Kaothien et al., 2005; Duan et al., 2010; Feiguelman et al., 2018; Liu et al., 2021; Lin et al.,
71   2022). ROP signalling pathways are mediated by plant-specific ROP GTPases, which are part
72   of the Rho family of small GTP-binding proteins that act as molecular switches and cycle
73   between an inactive GDP-bound state to an active GTP-bound state (Lin et al., 1996; Kost et
74   al., 1999b; Feiguelman et al., 2018). In their active state, ROPs interact with ROP
75   INTERACTING PARTNER (RIP) and ROP INTERACTING CRIB-CONTAINING PROTEIN
76   (RIC) proteins, which facilitate the specific activation of downstream pathways that are
77   required for polar growth (Holdaway-Clarke and Hepler, 2003; Shichrur and Yalovsky, 2006;
78   Nagawa et al., 2010; Steinhorst and Kudla, 2013; Feiguelman et al., 2018). During pollen tube
79   tip growth, ROPs are essential for cell polarisation and to promote tip growth (Lin et al., 1996;
80   Kost et al., 1999a). Recently, it was shown that ROP signalling is additionally crucial for pollen
81   germination, as the quadruple mutant *rop1;3;5;9* of all redundant, pollen-expressed ROPs is
82   sterile and incapable of pollen germination (Xiang et al., 2023). As ROP signalling is required
83   for pollen germination, we hypothesise that activators of ROP signalling are also crucial for
84   pollen germination. However, it is unknown which ROP activators are required for pollen
85   germination.

86   The activation of ROPs is stimulated by ROP-specific GUANINE EXCHANGE FACTORS
87   (ROPGEFs), which facilitate the exchange from GDP to GTP. *Arabidopsis thaliana* has 14 of
88   these ROPGEFs, hereafter called GEFs, which contain a conserved PLANT-SPECIFIC ROP
89   NUCLEOTIDE EXCHANGER (PRONE) domain and variable termini (Berken et al., 2005; Bos
90   et al., 2007; Zhang et al., 2010; Lin et al., 2012; Miyawaki and Yang, 2014). The PRONE
91   domain forms a homodimer in which each protein binds a ROP protein and catalyses the
92   nucleotide exchange of the GTPase, as demonstrated by the structure of ROP4 together with
93   the PRONE domain of GEF8 (Thomas et al., 2007; Berken and Wittinghofer, 2008). Individual
94   GEFs exhibit specific expression patterns and functions in different cell types and polarity
95   processes. We showed that GEF3, together with the previously known GEF4, is highly
96   expressed in root hairs and promotes polarity establishment or root hair growth (Duan et al.,
97   2010; Denninger et al., 2019). Specific GEFs are establishing the membrane domains required
98   for xylem development, and we showed that particular GEFs are expressed during phloem

99 differentiation (Nagashima et al., 2018; Roszak et al., 2021). Additionally to other processes, such as hormone signalling or pavement cell morphogenesis, GEFs were extensively studied in pollen tube tip growth (Kaothien et al., 2005; Zhang and McCormick, 2007; Yu et al., 2012; Chang et al., 2013; Feiguelman et al., 2018; Lin et al., 2022).

Of the 14 GEFs of *Arabidopsis thaliana*, multiple are expressed in mature pollen grains, and four are reliably detected in transcriptomic and proteomic approaches (Supplemental Figure S1) (Mergner et al., 2020). Previous studies mainly focused on GEF12 and investigated its role in growing pollen tubes and activating ROP signalling during tip growth. This showed that the activity of GEFs is promoted by phosphorylation of their C-termini by PRK RLKs or controlled by the cytosolic AGCVIII protein kinases AGC1.5 and AGC1.7, which phosphorylate the PRONE domain of GEFs. Overexpression or misregulation of GEFs resulted in a loss of polarity, pollen tube swelling, and unidirectional growth, while loss of GEF function led to shorter pollen tubes (Zhang and McCormick, 2007; Nagawa et al., 2010; Chang et al., 2013; Zhao et al., 2013; Li et al., 2018; Li et al., 2020). As for ROPs, redundancy between multiple GEFs was indicated during pollen tube growth. A *gef1/gef9/gef12/gef14* quadruple mutant displayed a mild reduction in pollen tube length, but only two of the mutated *GEFs* are expressed in pollen (Chang et al., 2013). Recently, a *gef8/gef9/gef11/gef12/gef13* quintuple mutant of all known pollen-expressed *GEFs* showed a decrease in pollen tube integrity during tip growth and reduced fertility (Zhou et al., 2023). These studies show the importance of GEFs in promoting and maintaining polar growth and, thus, male fertility. However, they only investigated pollen tube tip growth. The role of GEFs during pollen germination and which of these GEFs initiates and activates the growth process still need to be discovered.

Compared to the redundancy found among ROPs, GEFs can have specific functions during the establishment of a new polar domain and polar growth initiation. In root hairs, we showed that establishing the polar growth domain and tip growth are two processes activated by distinct GEFs. GEF3 is required to establish the root hair initiation domain and the polarisation of ROP2, while GEF4 drives the subsequent tip growth (Denninger et al., 2019). In pollen tube germination, a polar growth domain must be established quickly from a dormant cell to provide an advantage over competing pollen. Moreover, in Arabidopsis, this polar protein accumulation must be spatially flexible, as the area of pollen tube germination is not predetermined and is defined by the region in contact with the papilla cells (Edlund et al., 2004; Dresselhaus and Franklin-Tong, 2013). Therefore, pollen germination is a great model for studying the de novo formation of polar protein domains at the plasma membrane and understanding the spatiotemporal processes required to initiate polar growth. As GEF proteins have not been investigated during pollen germination, we investigated their role in this process to understand how GEFs activate ROP signalling in a spatiotemporally controlled manner to allow the *de novo* establishment of polar cellular growth.

136   We focused our research on the pollen-specific ROPGEFs (GEF8, GEF9, GEF11, GEF12,
137   and GEF13) during pollen germination (Mergner et al., 2020) and show that GEFs are
138   distinctively crucial for pollen germination and male fertility. We demonstrate that GEF8 and
139   GEF9, but not GEF11 and GEF12, form a transient polar domain at the plasma membrane of
140   the pollen germination site and that these GEFs drive polar ROP activation and cellular growth.
141   This novel subcellular localisation highlights that GEFs have specific roles during cellular
142   processes. Furthermore, this GEF accumulation appears in a biphasic temporal manner and
143   can shift its location. This is the first description of a polar domain with such flexibility, which
144   is crucial for polarity establishment, hence, pollen function and fertilisation success.

145

146   **Results**

147   **GEF8 and GEF9 biphasically accumulate at the pollen germination site**

148   In flowering plants, pollen germination is essential for male fertility and, thus, successful
149   double fertilisation. Therefore, it is crucial to understand the molecular mechanisms activating
150   pollen germination upstream of the essential ROP proteins (Xiang et al., 2023). Even though
151   multiple GEFs were shown to be involved in pollen tube growth, the GEFs involved in ROP
152   activation during pollen germination still need to be determined (Chang et al., 2013; Zhou et
153   al., 2023). To investigate the role of GEFs during pollen tube germination, we focused on five
154   GEF proteins (GEF8, GEF9, GEF11, GEF12, and GEF13) that had been found to be
155   expressed in mature pollen (Supplemental Figure S1) (Mergner et al., 2020). We fused these
156   five GEFs N-terminally with the yellow fluorescing protein mCitrine (mCit) under the control of
157   their endogenous promoter fragments to confirm their expression. We found mCit-GEF8,
158   mCit-GEF9, mCit-GEF11, and mCit-GEF12 signals in mature pollen, but no signal was
159   observed for mCit-GEF13 (Figure 1 and Supplemental Figure S2). We assessed mCit-GEF
160   localisation by live cell imaging in germinating pollen grains *in vitro* on pollen germination
161   medium (PGM) (Vogler et al. 2014). Shortly after imbibion on PGM, all GEFs showed a
162   similar localisation and were evenly distributed in the cytoplasm (Figure 1, Supplemental
163   Figure S2 and Supplemental Video 1-3). After several minutes of imbibion on PGM, we
164   observed that mCit-GEF8 and mCit-GEF9 accumulated at a defined region in the cell
165   periphery, which strongly correlated with the future germination site. Such an accumulation
166   was never observed for mCit-GEF11, mCit-GEF12, or mCit-GEF13 expressed under the
167   control of a *GEF12* promoter (Figure 1, Supplemental Figure S2, and Supplemental Video 1-
168   3, 19-20). This indicates a specific function of GEF8 and GEF9 during pollen germination
169   initiation. To further characterise this behaviour, we quantitatively compared the timing of
170   protein accumulation. We defined the first frame of a visibly emerged pollen tube as a
171   reference timepoint 0, with negative time points before and positive time points after this
172   reference point. By quantifying the timing of mCit-GEF8 and mCit-GEF9 accumulations using

173   multiple kymographs, we observed that both proteins showed a biphasic accumulation that,

174   on average, slightly differed between mCit-GEF8 and mCit-GEF9 (Figure 1A-D). The initial

175   accumulation of mCit-GEF8 and mCit-GEF9 started in a small region of the pollen grain

176   periphery and grew to 3-4 µm within, on average, 3 minutes for mCit-GEF8 and 5 minutes for

177   mCit-GEF9. The maximum of this initial accumulation was reached, on average, at timepoint

178   -11 min before germination for mCit-GEF8 and -9 min for mCit-GEF9, depicting a faster and

179   earlier accumulation of GEF8 compared to GEF9 (Figures 1C and 1D). However, it should be

180   noted that the timing of mCit-GEF8 accumulation was more consistent, which leads to a

181   clearer profile of the average intensity blot. In contrast, mCit-GEF9 accumulation was stronger

182   but less consistent in its timing, which causes a less concise profile of the average intensity

183   blot (Figures 1C and 1D). For mCit-GEF8 and mCit-GEF9, the timing of this initial

184   accumulation, which we considered the germination initiation, was variable, and the timepoint

185   of the maximal accumulation is specifically indicated (Figure 1A, "germination initiation"). The

186   overall timing and persistence of this protein accumulation can be observed in the

187   corresponding kymographs (Figure 1B). The initial accumulation of mCit-GEF8 and mCit-

188   GEF9 did not persist at the future germination site but disappeared after, on average, 3

189   minutes for mCit-GEF8 and 7 minutes for mCit-GEF9. Around the time of germination, we

190   observed a second accumulation of GEF8 and GEF9 around the initial accumulation site,

191   which also differed in timing between both proteins. mCit-GEF8 reaccumulated at timepoint -

192   2 min before pollen germination, while GEF9 accumulation started after germination (Figure

193   1C and 1D). This slightly different timing of the biphasic accumulation indicates that during the

194   initiation phase of pollen germination, either GEF8 or GEF9 are accumulated at the pollen

195   germination site. Interestingly, we observed that the second accumulation of mCit-GEF8/

196   mCit-GEF9 was sometimes slightly shifted laterally compared to the first accumulation before

197   germination. However, both sites were always near each other, indicating a certain flexibility

198   during the assembly of all required proteins of the tip growth machinery (Figure 1A and 1B

199   and Supplemental Video 1). Such flexibility of the polar growth domain is crucial for pollen

200   function, especially in species like *Arabidopsis thaliana*, in which the pollen apertures do not

201   predetermine the pollen germination site (Edlund et al., 2004). To confirm the accumulation

202   and timing of GEF8 and GEF9 compared to the evenly distributed GEF12, we simultaneously

203   observed mCit-GEF8 or mCit-GEF12 coexpressed with mScarlet-GEF9 (mSct-GEF9). mCit-

204   GEF8 and mSct-GEF9 both accumulated with a similar timing at the same location, confirming

205   the observations in the single marker lines. However, mCit-GEF12 was still evenly diffused in

206   the cytoplasm, with no significant accumulation when a clear accumulation of mSct-GEF9 was

207   visible (Figure 1E and 1F). These results show differences between individual GEFs, as mCit-

208   GEF11, mCit-GEF12, and mCit-GEF13 do not show specific localisations during pollen

209   germination, while mCit-GEF8 and mCit-GEF9 specifically accumulate at the pollen

210 germination site. Moreover, mCit-GEF8 and mCit-GEF9 show a similar but distinct biphasic

211 accumulation at the pollen germination site, with temporal differences between both proteins.

212 Taken together, the differential localisation during pollen germination indicates a specific and

213 subcellular localised role for GEF8 and GEF9 in initiating pollen germination.

214

215 **Distinct GEFs are required for pollen germination *in vitro***

216 In light of the specific accumulation of GEFs during pollen germination, we used loss-of-

217 function mutant lines to investigate the function of GEFs in pollen germination. We used available

218 T-DNA lines for *gef9-t1* (<u>GK-717A10</u>)*, gef11-t1 (SALK_126725), and gef12-t1*

219 *(SALK_103614)*, and generated CRISPR-Cas9 full-length deletion mutants, resulting in *gef8-*

220 *cΔ1, gef8-cΔ2, gef9-cΔ1, gef12-cΔ1* single mutants, and double mutants *gef8-Δc1/gef12-Δc1*

221 and *gef8c-Δ3/gef9-cΔ2* (Supplemental Figure S3). Col-0 was used as a wild-type reference

222 and reached a pollen germination efficiency of 84 % 4 hours after imbibition on PGM (Figure

223 2A-2B). *gef11-t1* (86 %) showed germination efficiencies similar to Col-0, while *gef9-t1* (79

224 %)*, gef12-t1* (70 %), and *gef12-cΔ1* (78 %) were slightly lower but not significantly different

225 from Col-0. In comparison to *gef9-t1*, *gef9-cΔ1* (55 %) showed a significant reduction of pollen

226 germination efficiency, indicating partial remaining GEF9 function in *gef9-t1*, which could be

227 explained by the location of the T-DNA insertion in the fifth intron. We excluded the presence

228 of full-length mRNA in *gef9-t1* by RT-PCR on flower cDNA and could only find partial *GEF9*

229 mRNA in front and behind the T-DNA insertion site (Supplemental Figure S3). The germination

230 efficiency of *gef8* CRISPR-Cas9 lines, *gef8-cΔ1* (63 %)*, and *gef8-cΔ2* (64 %) were

231 comparable to *gef9-cΔ1* and were significantly different from Col-0. We were able to rescue

232 *gef8-cΔ1* with the *GEF8p*::mCit-GEF8 construct, which led to a germination efficiency of 83%,

233 proving that the absence of GEF8 causes the phenotype and confirming the functionality of

234 the mCit-fusion constructs (Figure 2A). The pollen germination was more severely reduced in

235 *gef8-cΔ1;9-t1* (36 %) and *gef8-cΔ3;9-cΔ2* (50 %) double mutants, while *gef8-cΔ1;12-t1* (70

236 %) and *gef9-t1;12-t1* (66 %) double mutants displayed no significant reduction of germination

237 efficiency in comparison to the *gef8* and *gef9* single mutants. However, we still observed

238 significant pollen germination in *gef8;gef9* double mutants. Therefore, we generated a *gef8-*

239 *cΔ1;9-t1;12-t1* triple mutant. In this triple mutant line, *in vitro* pollen germination was almost

240 completely abolished (0.2 %), showing that these three GEFs are essential for pollen

241 germination (Figure 2A). In summary, this showed that GEF11 has no function in the pollen

242 germination of *Arabidopsis thaliana*. GEF8 and GEF9 play a major role in pollen germination,

243 as they both display a significant deficiency as single mutants, and this effect is amplified in

244 the double mutant. The normal pollen germination efficiency of GEF12 single mutants shows

245 a minor function of GEF12 in this process. However, because pollen germination was only

246 abolished in the combination of *gef8*, *gef9*, and *gef12*, a partial redundancy between these
247 three GEFs can be assumed.

248

249 **GEF function is crucial for efficient male fertility *in vivo***
250 After we showed the necessity of GEFs for pollen germination *in vitro*, we assessed their role
251 in pollination and male fertility *in vivo.* To determine the transmission efficiency of *gef* mutant
252 alleles, we performed reciprocal crosses using Col-0 with *gef8, gef9, and gef12* mutant
253 combination lines, in which one *gef* allele was heterozygous, leading to an expected
254 transmission of 50 % for this *gef* allele in the F1 offspring (Figure 2C and Supplemental Figure
255 S4). In the control direction with *gef* mutant lines as female, pollinated with Col-0 pollen, we
256 did not find any significant reduction in the transmission of the mutant alleles, showing that
257 *gef8*, *gef9*, and *gef12* are not required for female fertility (Supplemental Figure S4). When
258 using *gef* mutant lines for pollination, we did not see significant reductions from the expected
259 transmission *in gef8, gef9, and gef12* single and double mutant combinations. However, it
260 needs to be mentioned that we observed nonsignificant reductions of the allele frequency in
261 some *gef8/gef9* mutant allele combinations, which were not seen in other allele combinations
262 of the same genes (Figure 2C and Supplemental Figure S4). Only the triple mutant *gef8-*
263 *cΔ1;9-t1+/-;12-t1* had a reduced transmission of the *gef9-t1* allele (35 %), which significantly
264 differed from the expected 50 % (p=0.0004) transmission (Figure 2C and Supplemental Figure
265 S4). This effect on male fertility was lower than expected from the *in vitro* experiments but
266 confirmed that *GEF8, GEF9 and GEF12* are crucial for male fertility, likely by promoting
267 efficient pollen germination.

268

269 **The C-terminal domain is necessary and sufficient for GEF8 and GEF9 accumulation**
270 We showed that GEF8 and GEF9 have distinct localisation compared to GEF11 and GEF12.
271 To investigate which GEF proteins' components are responsible for this specificity, we
272 analysed different domains of GEFs during pollen germination. GEFs consist of a conserved
273 catalytic PRONE domain and variable N- and C-terminal regions. The existing crystal
274 structures of the PRONE domain of GEF8, together with ROP4, showed that these proteins
275 form a tetramer in which two GEFs dimerise, each having one ROP bound (Thomas et al.,
276 2007). However, the terminal regions of GEF8 were not represented in this structure, as they
277 are thought to be intrinsically disordered. Protein structure predictions of GEF8 and ROP1
278 using AlphaFold2 and matched on the existing PRONE8-ROP4 structure (RCSB-PDB: 2NTY)
279 with ChimeraX confirmed that these terminal regions are primarily unstructured, with only
280 small helical elements (Thomas et al., 2007; Mirdita et al., 2022; Meng et al., 2023). However,
281 in this predicted structure, both termini wrap around the protein, with the N-terminus blocking
282 the binding site of the second GEF and the C-terminus blocking the binding site of the ROP

283 (Figure 3A). This structure could explain the inhibitory function of both termini that was

284 described previously (Gu et al., 2006; Zhang and McCormick, 2007). We made several mutant

285 and deletion constructs to understand the function of GEF8 and GEF9 during pollen

286 germination and unravel the protein features responsible for their specific biphasic

287 accumulation (Figure 3B and 3C). We started by deleting the variable N-terminus of GEF8

288 (mCit-GEF8$^{\Delta N}$) and GEF9 (mCit-GEF9$^{\Delta N}$). The N-terminal deletion did not abolish the specific

289 localisation of either protein, as we could still observe an accumulation at the germination site

290 minutes before pollen tube emergence (Figure 3C Supplemental Video 4-5). Different effects

291 were observed in constructs in which the variable C-terminal region of GEF8 (mCit-GEF8$^{\Delta C}$)

292 and GEF9 (mCit-GEF9$^{\Delta C}$) was deleted. mCit-GEF8$^{\Delta C}$ and mCit-GEF9$^{\Delta C}$ were strictly cytosolic

293 and showed no membrane attachment during pollen germination. (Figure 3C and

294 Supplemental Video 6-7). This loss of accumulation of mCit-GEF8$^{\Delta C}$ and mCit-GEF9$^{\Delta C}$

295 showed that the GEF C-terminus is necessary for membrane attachment and the

296 accumulation of GEF8 and GEF9 during pollen germination. Because the C-terminal domain

297 is required for the accumulation of GEF8/GEF9 and this accumulation is not seen for mCit-

298 GEF12 throughout the pollen germination process, we swapped the C-terminal domain of

299 GEF12 with those of either GEF8 (mCit-GEF12^{GEF8C}) or GEF9 (mCit-GEF12^{GEF9C}) (Figure 3D

300 and Supplemental Video 8-9). GEF12^{GEF8C} and GEF12^{GEF9C} both accumulated at the pollen

301 germination site before pollen tube emergence, similar to the native mCit-GEF8 and mCit-

302 GEF9, which was never observed for wild-type mCit-GEF12. This showed that the C-terminal

303 domains of GEF8 and GEF9 are necessary for the polar accumulation of these proteins.

304 Moreover, both C-termini are sufficient to recruit other GEFs to the cell periphery of the future

305 pollen germination site.

306

307 **A phosphorylation site in the C-terminus of GEFs influences their accumulation**

308 To further understand the mechanism of GEF activation and localisation, we investigated the

309 role of phosphorylation in GEF8 and GEF9 C-terminal domains. The C-terminus of GEFs was

310 shown to be phosphorylated by RLKs at a serine of the conserved SPxxRH motif, leading to

311 the activation of the PRONE domain (Kaothien et al., 2005; Zhang and McCormick, 2007;

312 Cheung and Wu, 2008). The phosphorylation at this site was recently confirmed by proteomic

313 approaches (Mergner et al., 2020). In the predicted structure, this phosphorylation site is

314 accessible and could affect the blocking function of this domain (Figure 3E). To elucidate any

315 potential functional effect of the phosphorylation of this serine on pollen germination, we

316 mutated this serine to a phospho-dead (S518A) and potentially phospho-mimic (S518D)

317 versions of GEF8 and transformed them into the *gef8-cΔ1* background. Both mutants,

318 GEF8^{S518D} and GEF8^{S518A}, displayed no significant accumulation at the pollen tube

319 germination site (Figure 3E and Supplemental Video 10-11). This indicates that the protein

320 accumulation is independent of the activity status of GEF8, but rather, the phosphorylation
321 reaction by RLKs is critical for GEF accumulation. In summary, the deletion constructs of
322 GEF8 and GEF9, in combination with the domain swap experiments, show that the C-terminal
323 domain is necessary for the distinct accumulation of GEF8 and GEF9 and sufficient to transfer
324 this function onto GEF12, which usually does not accumulate in this system. In addition,
325 GEF8^{S518} seems to have an essential role in GEF8 accumulation at the germination site,
326 indicating that the activation by RLKs is a crucial factor in this process.

327

328 **GEF8 is necessary for ROP activation**
329 GEFs activate ROPs by exchanging GDP for GTP, leading to the recruitment of RIP or RIC
330 proteins and the subsequent activation of downstream processes (Feiguelman et al., 2018).
331 For example, RIC3 and RIC4 were shown to regulate pollen growth by mediating the
332 modulation of Ca^{2+} fluxes and F-actin formation (Theos et al., 2005). RICs contain a
333 CDC42/RAC INTERACTIVE BINDING (CRIB) motif, which mediates the interaction with
334 active GTP-bound ROPs. ROP1, ROP3, and ROP5 are specifically expressed in pollen grains.
335 We observed mCit-ROP1, mCit-ROP3, and mCit-ROP5 under their endogenous promoters,
336 and all three ROPs localised to the cytoplasm without any specific accumulation at the site of
337 germination, as observed for mCit-GEF8 and mCit-GEF9 (Figure 4A and 4B and
338 Supplemental Video 12-14). Nevertheless, as the CRIB domain is sufficient for active ROP
339 binding, it allows the utilisation of the CRIB domain as a biosensor for the localisation of active
340 ROPs (Luo et al., 2017). Here, we used the CRIB motif of RIC4 (CRIB4) fused to mCit under
341 the control of the *GEF12* promoter fragment (*GEF12p*::CRIB4-mCit) as an indicator of ROP
342 activity during pollen germination (Figure 4C and 4D). We observe a persistent CRIB4-mCit
343 accumulation at the germination site during the germination process, which differs from the
344 transient biphasic accumulation of mCit-GEF8 and mCit-GEF9 (Figure 4 and Supplemental
345 Video 15). However, the timing of the initiation of CRIB4-mCit accumulation was similar to the
346 one observed for both GEFs, approximately 10 minutes before germination. In addition, the
347 overall width of the accumulation of CRIB4-mCit was similar to that of mCit-GEF8 and mCit-
348 GEF9 (3-4 µm). To show the causality between the accumulation of GEF8 and CRIB4, we
349 investigated CRIB4-mCit localisation in a *gef8-cΔ1* background. In *gef8-cΔ1,* CRIB4-mCit
350 accumulation was lost, and its localisation is cytoplasmic, with no apparent accumulation at
351 the germination site during the pollen germination process (Figure 4C and Supplemental Video
352 16). These results suggest that CRIB4 (a biosensor for active ROPs) accumulates at the
353 germination site during the germination process, and this accumulation requires the activity of
354 GEF8, which shows a functional link between GEF8/9 accumulation and ROP activation.

355

GEF8 oscillation leads to changes in calcium oscillation

356 ROP signalling leads to the activation of downstream pathways required for pollen tube
357 growth, such as Ca^{2+} oscillations, which are essential for pollen tube growth and guidance
358 (Cheung and Wu, 2008; Dresselhaus et al., 2016; Gao et al., 2016). Ca^{2+} undergoes fine-
359 tuned oscillations and concentration variations to regulate polar growth (Iwano et al., 2009).
360 Ca^{2+} fluctuations are described during pollen germination *in vivo*, but their timing to other
361 activators of pollen germination and their cause during pollen activation still need to be
362 understood (Iwano et al., 2004). We used the Ca^{2+}-indicator RGeco1 under the control of the
363 *Lat52* promoter to monitor Ca^{2+} oscillations during pollen germination in Col-0 (Figure 4E and
364 Supplemental Video 17). Compared to the regular short oscillations during pollen tube growth,
365 we observed longer and persisting Ca^{2+} elevations. We found a first increase of Ca^{2+} around -
366 8 minutes before germination, which persisted with different intensities for multiple minutes,
367 decreased shortly before germination and increased again at timepoint 0 (Figure 4E and 4F).
368 This initial increase of Ca^{2+} was comparable to mCit-GEF8 and mCit-GEF9 accumulation,
369 indicating a possible interaction between GEF8/9 and Ca^{2+} elevations. To investigate the
370 association between GEF function and Ca^{2+} oscillation, we observed RGeco1 in *gef8-cΔ1*
371 during pollen germination (Figure 4E and Supplemental Video 18). Interestingly, the Ca^{2+}
372 elevation pattern was not abolished but differed from the one observed in Col-0. Compared to
373 Col-0, the RGeco1 signal did not increase in a persistent Ca^{2+} elevation in the *gef8-cΔ1* mutant
374 but rather showed several lower intensity peaks throughout the germination process, with one
375 stronger Ca^{2+} increase at the germination timepoint (Figure 4E and 4-F). This result further
376 emphasises the necessity of GEF8 for ROP activation, resulting in normal Ca^{2+} elevations and
377 pollen germination. In summary, the absence of GEF8 impacted CRIB4-mCit (active ROP
378 biosensor) and Ca^{2+} oscillations, showing the crucial function of GEFs in activating ROP
379 signalling leading to pollen germination.
380

381

382 **Discussion**

383 Pollen germination is a critical step in plant fertilisation, and characterising the underlying
384 protein functions is crucial for understanding the activation of this process. Here, we identified
385 specific ROPGEFs required for pollen germination and male fertility. These GEFs have distinct
386 functions during pollen germination, which are conferred, in parts, by their C-terminal domain.
387 Five of the 14 GEFs are expressed in mature Arabidopsis pollen (Supplemental Figure S1).
388 We confirmed the presence of GEF8, GEF9, GEF11, and GEF12 using translational fusion
389 lines but not GEF13 (Figure 1 and Supplemental Figure S2). As recent proteomics analysis
390 only found very low amounts of GEF13 in mature pollen, it remains unclear whether GEF13 is
391 irrelevant for pollen tube growth or is very specifically translated (Mergner et al., 2020).
392 Previous results also indicated the presence of GEF1 and GEF14 during pollen tube growth,

393 but the detection of the expression level of these two genes was found to be low and
394 inconsistent (Gu et al., 2006; Zhang and McCormick, 2007; Chang et al., 2013). In line with
395 this, *GEF1* and *GEF14* were not identified in recent transcriptomics or proteomics data
396 (Mergner et al., 2020).

397 The four consistently expressed GEFs have very distinct localisations, with GEF11 and GEF12
398 evenly distributed in the cytoplasm throughout the germination process, while GEF8 and GEF9
399 accumulated at the site of pollen germination before pollen tube growth (Figure 1 and
400 Supplemental Figure S2). A similar accumulation of GEFs was described for GEF3 and
401 GEF14 during root hair initiation (Denninger et al., 2019). However, during root hair initiation,
402 the polar domain requires around 30 minutes to be established, is locally fixed and is persistent
403 for hours (Denninger et al., 2019). The protein accumulations we observed for GEF8 and
404 GEF9 were established significantly faster but shorter, as they only persisted at the pollen
405 germination site for several minutes (Figure 1). An exciting aspect and a difference to the
406 initiation of root hair growth is that the localisation of GEF8 and GEF9 accumulation was not
407 fixed but could shift laterally during the initiation of pollen germination. This could be an
408 essential feature of polar growth in pollen, as these cells need to adjust the germination site
409 in response to contact with papilla cells. Thus, the flexibility of this growth machinery is
410 required to initiate growth at the optimal position in species such as *Arabidopsis thaliana* with
411 no predetermined germination site at the pollen apertures (Edlund et al., 2004). We also found
412 differences in the timing of protein accumulation between GEF8 and GEF9, leading to a
413 constant presence of GEF8 or GEF9 at the pollen germination site but with different ratios to
414 each other (Figure 1). It remains to be determined whether they have redundant functions at
415 this location or if distinct pathways are activated by these particular proteins, as described for
416 downstream RIC proteins (Gu et al., 2005).

417 The *gef8* and *gef9* single mutants had significantly reduced pollen germination efficiencies,
418 while *gef11* and *gef12* single mutants did not display significant reductions in pollen
419 germination (Figure 2 and Supplemental Figure S3). Compared to the previously postulated
420 redundancy of GEFs during pollen germination and growth, our results suggest, at least during
421 pollen germination, that individual GEFs have distinct localisations and non-redundant
422 functions (Chang et al., 2013; Zhou et al., 2023). The availability of suitable mutant lines can
423 explain the discrepancy with the previous reports, which did not detect the same defects, as
424 the observed phenotypes of *gef8* and *gef9* mutants were only evident in the CRISPR-Cas9
425 deletion mutants generated in this study (Figure 2 and Supplemental Figure S3). The only
426 available T-DNA line for *GEF8* had multiple T-DNA integrations and, in our experience,
427 showed developmental defects independent of the integration in *GEF8*. The available T-DNA
428 line of *GEF9* showed a mild and less consistent phenotype than the generated CRISPR-Cas9
429 deletion mutant (Figure 2 and Supplemental Figure S3). In combination with the presented

430 localisation data, our phenotyping analysis shows that not all GEFs act redundantly during
431 pollen germination. We suggest that these GEFs activate different aspects required for polar
432 growth to another degree. Thus, all GEFs are distinctively required for efficient pollen
433 germination and male fertility, which only leads to a severe phenotype in higher-order mutants
434 (Figure 2), similar to the observations made in loss-of-function mutants of all pollen-expressed
435 *ROPs* (Xiang et al., 2023). Additionally, the severity of the *gef8-cΔ1;9-t1;12-t1* triple mutant
436 phenotype observed *in vitro* can be overcome *in vivo*, as the *gef8-cΔ1;9-t1;12-t1* triple mutant,
437 which hardly showed pollen germination on PGM, still had a significant transmission in
438 reciprocal crosses (Figure 2C and Supplemental Figure S4), which is similar to recent data
439 shown in *gef8;9;11;12;13* quintuple mutants. Potentially, other GEFs might have a higher
440 activity *in vivo* that could rescue the lack of these primary GEFs, leading to a weaker
441 phenotype than the total loss of ROP activity (Xiang et al., 2023).
442 The distinct localisations we observed for GEF8 and GEF9 indicate that a specific feature of
443 those proteins transmits this function. As the PRONE domain of all GEFs is conserved, we
444 focused on the variable termini with no apparent structure and seeming intrinsically disordered
445 (Figure 3) (Berken et al., 2005). The predicted full-length structure of GEF8 suggests that both
446 termini are folding around the PRONE domain to either block ROP binding or prevent protein
447 dimerisation, indicating inhibitory functions. However, the confidence in the structure of these
448 regions is very low, and it remains unclear how these termini are folded or if they can take
449 different shapes depending on the situation. The N-terminus was shown to have activating
450 functions for GEF activity, while the C-terminus inhibits PRONE activity (Gu et al., 2006; Zhang
451 and McCormick, 2007). However, in contrast to the suggested function of the terminal domains
452 for GEF activity, we observed other functions for their localisation. The deletion of the N-
453 terminus did not significantly alter protein accumulation behaviour. In contrast, the deletion of
454 the C-terminus abolished protein accumulation (Figure 3C), which shows that the contribution
455 of the termini to protein activity and localisation independently regulates different aspects of
456 GEFs. We speculate that the C-terminus of GEF8 and GEF9 is required for interaction with
457 RLKs like PRKs, as shown before for GEF12, as mutations in the conserved phosphorylation
458 site can alter this accumulation (Figure 3) (Kaothien et al., 2005; Chang et al., 2013). However,
459 this interaction must be specific to GEF8 and GEF9 as we do not see such accumulations for
460 other GEFs. Moreover, the ability for protein accumulation before pollen tube emergence can
461 be transferred onto GEF12 when exchanging the C-terminal domain (Figure 3D). Suggesting
462 that other scaffolding proteins or other RLKs than the previously reported PRK2, PRK6, or
463 BUPS are responsible for this interaction, as they also interact with GEF12 (Chang et al.,
464 2013; Zhao et al., 2013; Takeuchi and Higashiyama, 2016; Yu et al., 2018; Zhou et al., 2021).
465 However, it is also possible that additional mechanisms are crucial for this accumulation or
466 that further factors transmit a specific interaction of GEF8 and GEF9 with the known RLKs at

467   this particular time during the initiation of pollen germination. Other proteins known to show

468   similar accumulation at the pollen germination site before germination are the ROP effector

469   scaffold proteins RIP1, RIC1, and potentially other members of these families or BOUNDARY

470   OF ROP DOMAIN (BDR) proteins. However, it is unlikely that these scaffolds drive GEF

471   accumulation, as they are ROP effectors, and their accumulation depends on ROP activation

472   (Li et al., 2008; Zhou et al., 2015; Sugiyama et al., 2019; Xiang et al., 2023). Still, these

473   effectors may have a role in stabilising the GEF accumulation in a feedback loop to confine

474   the domain, as shown in root hairs (Denninger et al., 2019).

475   The accumulation of GEFs did not lead to any significant accumulation of ROPs at the pollen

476   germination site (Figure 4A), which conforms with recent observations of ROPs during pollen

477   germination (Xiang et al., 2023). Still, we could observe that a marker for active ROPs and

478   Ca^{2+} signals are elevated at the pollen germination site with a timing similar to the observed

479   GEF accumulations. In line with this, the accumulation of the active ROP marker was lost, and

480   the Ca^{2+} elevation pattern was altered in the *gef8-cΔ1* mutant (Figure 4C and 4D). The

481   complete loss of accumulation of the ROP activity indicator (CRIB domain) is surprising,

482   considering the mild phenotype in *gef8-cΔ* mutants (Figure 2). However, the accumulation of

483   this indicator is also very low, and it might be that slight changes in ROP activity already have

484   significant effects on this sensor, even though the remaining ROP activity is sufficient to trigger

485   altered Ca^{2+} signals and induce pollen germination. However, this alteration of ROP activity in

486   *gef* mutants indicates that GEF accumulation is upstream of ROP activity and requires a

487   different mechanism. A connection to phospholipid signalling is possible, as shown in root

488   cells (Platre et al., 2019). Candidate proteins are PHOSPHATIDYLINOSITOL 4-PHOSPHATE

489   5-KINASEs (PIP4Ks) that regulate phospholipid abundance and regulate tip growth in pollen

490   tubes and root hair cells (Kusano et al., 2008; Kato et al., 2024). PIP4Ks also accumulate at

491   the pollen germination site and might act together with GEFs to drive ROP signalling, but

492   results in root hairs suggest that PIP4K accumulation is downstream of GEF accumulation

493   (Denninger et al., 2019; Kato et al., 2024). Still, studying the connection to other pathways and

494   their regulatory connection will be a challenging task to fully understand polarity establishment

495   and polar growth initiation.

496   We show that specific GEFs are required for efficient pollen germination and that GEF8 and

497   GEF9 display distinct localisations compared to GEF11 and GEF12. Together, this shows that

498   GEFs are not redundant during pollen germination and can have specific functions within the

499   same process in one cell. The novel polar domain of accumulated GEF8/9 protein in

500   germinating pollen tubes was spatiotemporally flexible and not static as in previously

501   described processes. We hypothesise that this flexibility is crucial to define the pollen

502   germination site independently of predeterminant features and shows the *de novo* assembly

503   of a polar growth domain.

504 **Material and Methods**

505

506 **Plant material and growth conditions:**

507 *Arabidopsis thaliana* plants were grown on soil under long-day conditions (16 h of light at 21 C)

508 in a growth chamber. *Arabidopsis thaliana* ecotype Col-0 was used as a wild-type reference.

509 The mutant lines *gef9-t1* (GK-717A10), *gef11-t1* (SALK_126725C), and *gef12-t1*

510 (SALK_103614) were obtained from NASC (Nottingham Arabidopsis Stock Centre). Single

511 t-DNA insertion was confirmed by segregation analysis, and the t-DNA insertion site was

512 checked by sequencing the genotyping PCR product on both sides of the insertion site.

513 Primers used for genotyping are listed in Supplemental Table S1. Double and triple mutants

514 were made by crossing these lines and were selected by PCR. Fluorescently labelled

515 *GEF12p*::mCit-GEF12 was used from (Denninger et al., 2019).

516

517 **CRISPR/Cas9 deletion lines:**

518 To generate *gef8-cΔ1* and *gef12-cΔ1* CRISPR/Cas9 deletion lines, we used an egg cell-

519 specific promoter-driven CRISPR/Cas9 (Wang et al., 2015). We used two gRNAs, one in 5'

520 and the other in 3' of the gene, cloned in tandem into one vector (Supplemental Figure S3).

521 The selection of positive transformants in T1 generation was done on ½ MS medium

522 containing Hygromycin (20 μg/ml).

523 To generate CRISPR/Cas9 deletion lines for *gef8-cΔ2* (2.2kb) and *gef9-cΔ1* (2.7kb) single

524 mutants and *gef8c-Δ3/gef9-cΔ2* double mutants, we used a multiplex editing approach based

525 on an optimised zCas9i (Stuttmann et al., 2021). We used four gRNAs per gene, two in 5' and

526 two in 3' of the gene. (Supplemental Figure S3). The selection of positive lines in T1 was

527 performed using seed fluorescence and Basta resistance. T2 selection was made by selecting

528 non-glowing seeds.gRNAs were determined using ChopChop (https://chopchop.cbu.uib.no/)

529 (Labun et al., 2019) and CCTop (https://cctop.cos.uni-heidelberg.de/) (Stemmer et al., 2015)

530 and successful cloning was confirmed by sequencing. Genotyping was performed by primers

531 200-300bp outside the deleted area. The characterisation of the deletion was done by

532 sequencing the resulting PCR product. Confirmation of homozygous mutant alleles was done

533 by combination with a primer binding in the deleted region and was confirmed in the following

534 generation. All primers are listed in Supplemental Table S1.

535

536 **Plasmid construct:**

537 All non-CRISPR/Cas9 constructs were generated using the GreenGate cloning system

538 (Lampropoulos et al., 2013) with modified cloning procedures. A list of combined modules and

539 their sources is provided in Supplemental Table S2. As native promoter sequences upstream

540 regions of the START codon, including the 5'UTRs, were cloned for *GEF8* (AT3G24620, -

541   2501bp), *GEF9* (AT4G13240, -1463bp), *GEF11* (AT1G52240, -973bp), *GEF12* (AT1G79860,

542   701bp), and *GEF13* (AT3G16130, 850bp and 1200pb) The *LAT52* promoter was amplified

543   from LHR lines (Denninger et al., 2014) and a RGeco1 module was kindly provided by Rainer

544   Waadt (Waadt et al., 2017) The CRIB4 module was generated by amplification of the CRIB

545   domain of RIC4 (AT5G16490, amino acid I64-I131) as described before (Luo et al., 2017) from

546   flower cDNA. All primers used to generate new Entry-Vector modules are listed in

547   Supplemental Table S1. The correct amplification and cloning of entry-vector modules were

548   confirmed by sequencing. We generated a new GreenGate-compatible destination vector to

549   achieve a higher plant transformation efficiency. For this, we amplified the vector backbone of

550   pHEE401E (Wang et al., 2015) and the GreenGate cloning cassette of pGGZ003

551   (Lampropoulos et al., 2013) by PCR (Primers in Supplemental Table S1) and combined both

552   fragments using added MluI and BamHI sites. The resulting plasmid was confirmed by

553   sequencing and named pGGX000.

554

555   **Phenotyping of pollen germination efficiency:**

556   For phenotyping of *in vitro* pollen germination efficiency, pollen of freshly opened flowers was

557   germinated at 22°C on solid pollen germination medium (PGM), containing 1.5% agarose

558   (w/v), 18% sucrose (w/v), 0.01% boric acid (w/v), 1mM $CaCl_2$, 1mM $Ca(NO3)_2$, 1mM $MgSO_4$,

559   10µM 24-epibrassinolides (MedChemExpress, HY-N084824, dissolved to 5mM in Ethanol),

560   and adjusted to pH=7.0 using 100 mM KOH,) (Vogler *et al.*, 2014). Germination was analysed

561   4 hours after imbibition on the PGM, using a Leica MZ16 stereomicroscope equipped with

562   DMC5400. The images were analysed using the multipoint tool of ImageJ

563   (https://imagej.nih.gov/ij/docs/guide/146-19.html#sec:Multi-point-Tool), then making the ratio

564   of germinated and ungerminated pollen to get the germination efficiency. Each line was

565   analysed in at least three independent experiments, including three replicates in each

566   experiment. Each data point represents an independent replicate analysing more than 150

567   pollen grains. Statistical analysis was performed using GraphPad Prism 9. We used a one-

568   way ANOVA with a post-Tukey test (significance level <0.0001) to test for significant

569   differences in pollen germination efficiency.

570

571   **Fluorescence imaging and quantification:**

572   Imaging of *in vitro* pollen germination was done at 22°C on solid PGM, containing 1.5%

573   agarose (w/v, 10% sucrose (w/v), 0.01% boric acid (w/v), 5mM $CaCl_2$, 5mM KCl, 1mM $MgSO_4$,

574   adjusted to pH=7.5 using 100 mM KOH (Boavida and McCormick, 2007) and supplemented

575   with 10µM 24-epibrassinolides (MedChemExpress, HY-N084824, dissolved to 5mM in

576   Ethanol) (Vogler et al., 2014).

577 Live cell imaging was performed using an Olympus confocal FV-1000 equipped with a 40x
578 water immersion (1.15 NA) objective, an Argon laser, and a 559 nm diode laser. Signals were
579 detected with high-sensitivity detectors. mCitrine (YFP) was excited at 515 nm and detected
580 between 520-550nm. mScarlet (RFP) and RGeco signals were exited at 559 nm and were
581 detected between 580-653 nm. The pinhole was set to 1AU, and images were taken with a 2x
582 line average in a 1024x1024 pixel scanning field. The same settings were applied to all
583 images, and the excitation laser intensity was set to a minimum for the individual lines to avoid
584 phototoxicity. GEF live pollen germination images were acquired every 30 seconds for 30
585 minutes. For Lat52p::RGeco, images were acquired every 5 seconds for 30 minutes. The
586 images were processed and analysed using ImageJ. Kymographs were generated with the
587 MultipleKymograph plugin, using a line width of five pixels.

588
589
590

591 **Acknowledgements**

600
601

602 **Author contributions**

603 P.D. conceived the study; A.M.B. and P.D. performed experiments, analysed data, prepared
604 figures, and wrote the manuscript with input from A.L.; A.M.B., A.L. and P.D. generated
605 experimental material; All authors read and approved the final version of the manuscript.

606
607

References

608

609 **Berken A, Thomas C, Wittinghofer A** (2005) A new family of RhoGEFs activates the Rop
610   molecular switch in plants. Nature **436**: 1176–1180

611 **Berken A, Wittinghofer A** (2008) Structure and function of Rho-type molecular switches in
612   plants. Plant Physiol Biochem **46**: 380–393

613 **Bleckmann A, Alter S, Dresselhaus T** (2014) The beginning of a seed: regulatory
614   mechanisms of double fertilization. Front Plant Sci **5**: 452

615 **Boavida LC, McCormick S** (2007) Temperature as a determinant factor for increased and
616   reproducible in vitro pollen germination in Arabidopsis thaliana. Plant J **52**: 570–582

617 **Boisson-Dernier A, Roy S, Kritsas K, Grobei MA, Jaciubek M, Schroeder JI,**
618   **Grossniklaus U** (2009) Disruption of the pollen-expressed FERONIA homologs ANXUR1
619   and ANXUR2 triggers pollen tube discharge. Development **136**: 3279–3288

620 **Bos JL, Rehmann H, Wittinghofer A** (2007) GEFs and GAPs: Critical Elements in the
621   Control of Small G Proteins (DOI:10.1016/j.cell.2007.05.018). Cell **130**: 385

622 **Chang F, Gu Y, Ma H, Yang Z** (2013) AtPRK2 Promotes ROP1 Activation via RopGEFs in
623   the Control of Polarized Pollen Tube Growth. Mol Plant **6**: 1187–1201

624 **Cheung AY, Wu HM** (2008) Structural and signaling networks for the polar cell growth
625   machinery in pollen tubes. Annu Rev Plant Biol **59**: 547–572

626 **Denninger P, Bleckmann A, Lausser A, Vogler F, Ott T, Ehrhardt DW, Frommer WB,**
627   **Sprunck S, Dresselhaus T, Grossmann G** (2014) Male–female communication triggers
628   calcium signatures during fertilization in Arabidopsis. Nat Commun **5**: 4645

629 **Denninger P, Reichelt A, Schmidt VAF, Mehlhorn DG, Asseck LY, Stanley CE, Keinath**
630   **NF, Evers J-F, Grefen C, Grossmann G** (2019) Distinct RopGEFs Successively Drive
631   Polarization and Outgrowth of Root Hairs. Curr Biol **29**: 1854-1865.e5

632 **Dresselhaus T, Franklin-Tong N** (2013) Male-female crosstalk during pollen germination,
633   tube growth and guidance, and double fertilization. Mol Plant **6**: 1018–1036

634 **Dresselhaus T, Sprunck S, Wessel GM** (2016) Fertilization mechanisms in flowering plants.
635   Curr Biol **26**: R125–R139

636 **Duan Q, Kita D, Li C, Cheung AY, Wu H-M** (2010) FERONIA receptor-like kinase regulates
637   RHO GTPase signaling of root hair development. Proc Natl Acad Sci **107**: 17821–17826

638 **Edlund AF, Swanson R, Preuss D** (2004) Pollen and stigma structure and function: the role
639   of diversity in pollination. Plant Cell **16 Suppl**: S84-97

640 **Feiguelman G, Fu Y, Yalovsky S** (2018) ROP GTPases Structure-Function and Signaling
641   Pathways. Plant Physiol **176**: 57–79

642 **Gao QF, Gu LL, Wang HQ, Fei CF, Fang X, Hussain J, Sun SJ, Dong JY, Liu H, Wang YF**
643   (2016) Cyclic nucleotide-gated channel 18 is an essential Ca2+ channel in pollen tube tips
644   for pollen tube guidance to ovules in Arabidopsis. Proc Natl Acad Sci U S A **113**: 3096–
645   3101

646 **Ge Z, Bergonci T, Zhao Y, Zou Y, Du S, Liu M-C, Luo X, Ruan H, García-Valencia LE,**
647   **Zhong S, et al** (2017) Arabidopsis pollen tube integrity and sperm release are regulated
648   by RALF-mediated signaling. Science **358**: 1596–1600

649 **Gu Y, Fu Y, Dowd P, Li S, Vernoud V, Gilroy S, Yang Z** (2005) A Rho family GTPase
650   controls actin dynamics and tip growth via two counteracting downstream pathways in
651   pollen tubes. J Cell Biol **169**: 127–138

652 **Gu Y, Li S, Lord EM, Yang Z** (2006) Members of a Novel Class of Arabidopsis Rho Guanine
653   Nucleotide Exchange Factors Control Rho GTPase-Dependent Polar Growth. Plant Cell
654   **18**: 366–381

655 **Hamamura Y, Nishimaki M, Takeuchi H, Geitmann A, Kurihara D, Higashiyama T** (2014)
656   Live imaging of calcium spikes during double fertilization in Arabidopsis. Nat Commun **5**:
657   4722

Holdaway-Clarke TL, Hepler PK (2003) Control of pollen tube growth: role of ion gradients and fluxes. New Phytol **159**: 539–563

Iwano M, Entani T, Shiba H, Kakita M, Nagai T, Mizuno H, Miyawaki A, Shoji T, Kubo K, Isogai A, et al (2009) Fine-tuning of the cytoplasmic Ca2+ concentration is essential for pollen tube growth. Plant Physiol **150**: 1322–1334

Iwano M, Shiba H, Miwa T, Che F-S, Takayama S, Nagai T, Miyawaki A, Isogai A (2004) Ca2+ Dynamics in a Pollen Grain and Papilla Cell during Pollination of Arabidopsis. Plant Physiol **136**: 3562–3571

Kaothien P, Ok SH, Shuai B, Wengier D, Cotter R, Kelley D, Kiriakopolos S, Muschietti J, McCormick S (2005) Kinase partner protein interacts with the LePRK1 and LePRK2 receptor kinases and plays a role in polarized pollen tube growth. Plant J **42**: 492–503

Kato M, Watari M, Tsuge T, Zhong S, Gu H, Qu L, Fujiwara T, Aoyama T (2024) Redundant function of the Arabidopsis phosphatidylinositol 4-phosphate 5-kinase genes PIP5K4–6 is essential for pollen germination. Plant J **117**: 212–225

Kost B, Lemichez E, Spielhofer P, Hong Y, Tolias K, Carpenter C, Chua N-H (1999a) Rac Homologues and Compartmentalized Phosphatidylinositol 4, 5-Bisphosphate Act in a Common Pathway to Regulate Polar Pollen Tube Growth. J Cell Biol **145**: 317–330

Kost B, Lemichez E, Spielhofer P, Hong Y, Tolias K, Carpenter C, Chua N (1999b) Tube Growth. J Cell Biol **145**: 317–330

Kusano H, Testerink C, Vermeer JEM, Tsuge T, Shimada H, Oka A, Munnik T, Aoyama T (2008) The Arabidopsis Phosphatidylinositol Phosphate 5-Kinase PIP5K3 Is a Key Regulator of Root Hair Tip Growth. Plant Cell **20**: 367–380

Labun K, Montague TG, Krause M, Torres Cleuren YN, Tjeldnes H, Valen E (2019) CHOPCHOP v3: Expanding the CRISPR web toolbox beyond genome editing. Nucleic Acids Res **47**: W171–W174

Lampropoulos A, Sutikovic Z, Wenzl C, Maegele I, Lohmann JU, Forner J (2013) GreenGate - A novel, versatile, and efficient cloning system for plant transgenesis. PLoS One **8**: e83043

Li E, Cui Y, Ge F-RR, Chai S, Zhang W-TT, Feng Q-NN, Jiang L, Li S, Zhang Y (2018) AGC1.5 Kinase Phosphorylates RopGEFs to Control Pollen Tube Growth. Mol Plant **11**: 1198–1209

Li E, Zhang YY-L, Shi X, Li H, Yuan X, Li S, Zhang YY-L (2020) A positive feedback circuit for ROP-mediated polar growth. Mol Plant **14**: 108947

Li S, Gu Y, Yan A, Lord E, Yang ZB (2008) RIP1 (ROP Interactive Partner 1)/ICR1 marks pollen germination sites and may act in the ROP1 pathway in the control of polarized pollen growth. Mol Plant **1**: 1021–1035

Lin D, Nagawa S, Chen J, Cao L, Chen X, Xu T, Li H, Dhonukshe P, Yamamuro C, Friml J, et al (2012) A ROP GTPase-Dependent Auxin Signaling Pathway Regulates the Subcellular Distribution of PIN2 in Arabidopsis Roots. Curr Biol **22**: 1319–1325

Lin W, Tang W, Pan X, Huang A, Gao X, Anderson CT, Yang Z (2022) Arabidopsis pavement cell morphogenesis requires FERONIA binding to pectin for activation of ROP GTPase signaling. Curr Biol **32**: 497-507.e4

Lin Y, Wang Y, Zhu J, Yang Z (1996) Localization of a Rho GTPase Implies a Role in Tip Growth and Movement of the Generative Cell in Pollen Tubes. Plant Cell **8**: 293

Liu C, Shen L, Xiao Y, Vyshedsky D, Peng C, Sun X, Liu Z, Cheng L, Zhang H, Han Z, et al (2021) Pollen PCP-B peptides unlock a stigma peptide–receptor kinase gating mechanism for pollination. Science **372**: 171–175

Luo N, Yan A, Liu G, Guo J, Rong D, Kanaoka MM, Xiao Z, Xu G, Higashiyama T, Cui X, et al (2017) Exocytosis-coordinated mechanisms for tip growth underlie pollen tube growth guidance. Nat Commun **8**: 1687

708 **Meng EC, Goddard TD, Pettersen EF, Couch GS, Pearson ZJ, Morris JH, Ferrin TE** (2023)
709   UCSF ChimeraX: Tools for structure building and analysis. Protein Sci **32**: e4792

710 **Mergner J, Frejno M, List M, Papacek M, Chen X, Chaudhary A, Samaras P, Richter S,**
711   **Shikata H, Messerer M, et al** (2020) Mass-spectrometry-based draft of the Arabidopsis
712   proteome. Nature **579**: 409–414

713 **Mirdita M, Schütze K, Moriwaki Y, Heo L, Ovchinnikov S, Steinegger M** (2022) ColabFold:
714   making protein folding accessible to all. Nat Methods **19**: 679–682

715 **Miyawaki KN, Yang Z** (2014) Extracellular signals and receptor-like kinases regulating ROP
716   GTPases in plants. Front Plant Sci **5**: 449

717 **Miyazaki S, Murata T, Sakurai-Ozato N, Kubo M, Demura T, Fukuda H, Hasebe M** (2009)
718   ANXUR1 and 2, sister genes to FERONIA/SIRENE, are male factors for coordinated
719   fertilization. Curr Biol **19**: 1327–1331

720 **Mu JH, Lee HS, Kao TH** (1994) Characterization of a pollen-expressed receptor-like kinase
721   gene of Petunia inflata and the activity of its encoded kinase. Plant Cell **6**: 709–721

722 **Muschietti J, Eyal Y, McCormick S** (1998) Pollen Tube Localization Implies a Role in Pollen–
723   Pistil Interactions for the Tomato Receptor-like Protein Kinases LePRK1 and LePRK2.
724   Plant Cell **10**: 319–330

725 **Nagashima Y, Tsugawa S, Mochizuki A, Sasaki T, Fukuda H, Oda Y** (2018) A Rho-based
726   reaction-diffusion system governs cell wall patterning in metaxylem vessels. Sci Rep **8**:
727   11542

728 **Nagawa S, Xu T, Yang Z** (2010) RHO GTPase in plants. Small GTPases **1**: 78–88

729 **Platre MP, Bayle V, Armengot L, Bareille J, Marquès-Bueno MDM, Creff A, Maneta-**
730   **Peyret L, Fiche J-B, Nollmann M, Miège C, et al** (2019) Developmental control of plant
731   Rho GTPase nano-organization by the lipid phosphatidylserine. Science **364**: 57–62

732 **Roszak P, Heo J, Blob B, Toyokura K, Sugiyama Y, de Luis Balaguer MA, Lau WWY,**
733   **Hamey F, Cirrone J, Madej E, et al** (2021) Cell-by-cell dissection of phloem development
734   links a maturation gradient to cell specialization. Science **374**: eaba5531

735 **Rudall PJ, Bateman RM** (2007) Developmental bases for key innovations in the seed-plant
736   microgametophyte. Trends Plant Sci **12**: 317–326

737 **Shichrur K, Yalovsky S** (2006) Turning ON the switch - RhoGEFs in plants. Trends Plant Sci
738   **11**: 57–59

739 **Sprunck S** (2020) Twice the fun, double the trouble: gamete interactions in flowering plants.
740   Curr Opin Plant Biol **53**: 106–116

741 **Steinhorst L, Kudla J** (2013) Calcium - a central regulator of pollen germination and tube
742   growth. Biochim Biophys Acta - Mol Cell Res **1833**: 1573–1581

743 **Stemmer M, Thumberger T, Del Sol Keyer M, Wittbrodt J, Mateo JL** (2015) CCTop: An
744   intuitive, flexible and reliable CRISPR/Cas9 target prediction tool. PLoS One **10**: 1–11

745 **Stuttmann J, Barthel K, Martin P, Ordon J, Erickson JL, Herr R, Ferik F, Kretschmer C,**
746   **Berner T, Keilwagen J, et al** (2021) Highly efficient multiplex editing: one-shot generation
747   of 8× Nicotiana benthamiana and 12× Arabidopsis mutants. Plant J **106**: 8–22

748 **Sugiyama Y, Nagashima Y, Wakazaki M, Sato M, Toyooka K, Fukuda H, Oda Y** (2019) A
749   Rho-actin signaling pathway shapes cell wall boundaries in Arabidopsis xylem vessels. Nat
750   Commun **10**: 1–7

751 **Takeuchi H, Higashiyama T** (2016) Tip-localized receptors control pollen tube growth and
752   LURE sensing in Arabidopsis. Nature **531**: 245–8

753 **Tang W, Kelley D, Ezcurra I, Cotter R, McCormick S** (2004) LeSTIG1, an extracellular
754   binding partner for the pollen receptor kinases LePRK1 and LePRK2, promotes pollen tube
755   growth in vitro. Plant J **39**: 343–353

756

757

Theos AC, Martina A, Hurbain I, Peden AA, Sviderskaya E V, Stewart A, Robinson MS, Bennett DC, Cutler DF, Bonifacino JS, et al (2005) Functions of adaptor protein (AP)-3 and AP-1 in tyrosinase sorting from endosomes to melanosomes. Mol Biol Cell **16**: 5356–5372

Thomas C, Fricke I, Scrima A, Berken A, Wittinghofer A (2007) Structural Evidence for a Common Intermediate in Small G Protein-GEF Reactions. Mol Cell **25**: 141–149

Vogler F, Schmalzl C, Englhart M, Bircheneder M, Sprunck S (2014) Brassinosteroids promote Arabidopsis pollen germination and growth. Plant Reprod **27**: 153–167

Waadt R, Krebs M, Kudla J, Schumacher K (2017) Multiparameter imaging of calcium and abscisic acid and high-resolution quantitative calcium measurements using R-GECO1-mTurquoise in Arabidopsis. New Phytol **216**: 303–320

Wang ZP, Xing HL, Dong L, Zhang HY, Han CY, Wang XC, Chen QJ (2015) Egg cell-specific promoter-controlled CRISPR/Cas9 efficiently generates homozygous mutants for multiple target genes in Arabidopsis in a single generation. Genome Biol **16**: 1–12

Xiang X, Zhang S, Li E, Shi X-L, Zhi J-Y, Liang X, Yin G-M, Qin Z, Li S, Zhang Y (2023) RHO OF PLANT proteins are essential for pollen germination in Arabidopsis. Plant Physiol 0–2

Yu F, Qian L, Nibau C, Duan Q, Kita D, Levasseur K, Li X, Lu C, Li H, Hou C, et al (2012) FERONIA receptor kinase pathway suppresses abscisic acid signaling in Arabidopsis by activating ABI2 phosphatase. Proc Natl Acad Sci **109**: 14693–14698

Yu Y, Song J, Tian X, Zhang H, Li L, Zhu H (2018) Arabidopsis PRK6 interacts specifically with AtRopGEF8/12 and induces depolarized growth of pollen tubes when overexpressed. Sci China Life Sci **61**: 100–112

Zhang C, Kotchoni SO, Samuels AL, Szymanski DB (2010) SPIKE1 signals originate from and assemble specialized domains of the endoplasmic reticulum. Curr Biol **20**: 2144–2149

Zhang Y, McCormick S (2007) A distinct mechanism regulating a pollen-specific guanine nucleotide exchange factor for the small GTPase Rop in Arabidopsis thaliana. Proc Natl Acad Sci **104**: 18830–18835

Zhao X-Y, Wang Q, Li S, Ge F-R, Zhou L-Z, McCormick S, Zhang Y (2013) The juxtamembrane and carboxy-terminal domains of Arabidopsis PRK2 are critical for ROP-induced growth in pollen tubes. J Exp Bot **64**: 5599–5610

Zhou X, Han W, Dai J, Liu S, Gao S, Guo Y, Xu T, Zhu X (2023) SPA, a Stigma-style-transmitting tract Physical microenvironment Assay for investigating mechano-signaling in pollen tubes. Proc Natl Acad Sci **120**: 2017

Zhou X, Lu J, Zhang Y, Guo J, Lin W, Van Norman JM, Qin Y, Zhu X, Yang Z (2021) Membrane receptor-mediated mechano-transduction maintains cell integrity during pollen tube growth within the pistil. Dev Cell **56**: 1030-1042.e6

Zhou Z, Shi H, Chen B, Zhang R, Huang S, Fu Y (2015) Arabidopsis RIC1 Severs Actin Filaments at the Apex to Regulate Pollen Tube Growth. Plant Cell **27**: 1140–1161

798 **Figures**

799

800 **Figure 1: GEF8 and GEF9 specifically accumulate at the pollen germination site before**
801 **germination initiation.**

802 (**A**) Protein localisation of mCit-GEF8, mCit-GEF9, and mCit-GEF12 under their respective
803 promoters during pollen germination. Timepoint 0 corresponds to the beginning of pollen tube
804 emergence, arrowheads mark the site of pollen emergence, and asterisks mark mCit-GEF9
805 localisation around the sperm cells. (**B**) Kymographs of time-lapse images corresponding to
806 (A) along a line crossing the pollen through the germination site (left) or around the pollen
807 grain (right). The dotted line indicates Timepoint 0 of pollen tube emergence; arrowheads
808 highlight protein accumulations at the pollen germination site. (**C** & **D**) Average intensity
809 profiles of mCit-GEF8 (n=13) and mCit-GEF9 (n=12) at the pollen germination site in relation
810 to the opposite side of the pollen grain during pollen germination. (**E** & **F**) Colocalization (left)
811 and intensity profiles along a line, as indicated in the merged image, across the pollen grain
812 through the pollen germination site (right) of mCit-GEF8 with mSct-GEF9 (E) and mCit-GEF12
813 with mSct-GEF9 (F) expressed under their respective promoters. All scale bars represent 10
814 µm.

815

816 **Figure 2: GEF8, GEF9, and GEF12 are necessary for pollen germination and male**
817 **fertility.**

818 (**A**) Quantification of pollen germination efficiency of *in vitro* germinated pollen 4 h after
819 imbibition on pollen germination media (PGM). Each point represents one replicate with more
820 than 150 pollen grains. Tukey's multiple comparison test was performed by one-way ANOVA,
821 and groups of statistically significant differences are indicated with letters ($p < 0.0001$). (**B**)
822 Representative images of *in vitro* germinated pollen 4 h after imbibition on PGM. (**C**)
823 Quantification of mutant allele frequency in F1 generation of reciprocal crosses with Col-0 as
824 female and the indicated mutants as pollen donors. The heterozygous allele of each genotype
825 is indicated in bold. Asterisks indicate a significant difference in the allele frequency from the
826 expected 50% according to X^2-test ($p < 0.05$).

827

828 **Figure 3: The C-terminus of GEF8 and GEF9 is necessary and sufficient for protein**
829 **accumulation.**

830 (**A**) AlphaFold2 protein structure prediction of full-length GEF8 and ROP1 (Rank 1, predicted
831 separately), matched on the PRONE8-ROP4 double-dimer structure (PDB: 2NTY). Different
832 angles are shown, and the terminal regions are indicated with different colours. (**B**) Schemes
833 of GEF protein structure and investigated truncation constructs, with variable N and C terminal
834 domains indicated as in (A). (**C** – **E**) Protein localisation of different mutant constructs under

their respective promoters during pollen germination. Timepoint 0 corresponds to the beginning of pollen tube emergence, arrowheads mark the site of pollen emergence, and asterisks mark localisation around the sperm cells. (**C**) Truncation constructs mCit-GEF8$^{\Delta N}$, mCit-GEF8$^{\Delta C}$, mCit-GEF9$^{\Delta N}$, and mCit-GEF9$^{\Delta C}$ in Col-0. (**D**) Domain swap constructs of GEF12 with alternative C-terminal domain, mCit-GEF12^{GEF8C} and mCit-GEF12^{GEF9C} in Col-0. (**E**) Phosphorylation site mutations of GEF8-S518 to a phospho-mimic (mCit-GEF8^{S518D}) and phospho-dead variant (mCit-GEF8^{S518A}) variant expressed in *gef8-cΔ1*. All scale bars represent 10μm.

Figure 4: GEF8 is required for polar ROP activation and Ca^{2+} signalling.

(**A**) Localization of mCit-ROP1, mCit-ROP3, and mCit-ROP5 under their respective promoter during pollen germination. Timepoint 0 corresponds to the beginning of pollen tube emergence, and arrowheads mark the site of pollen emergence. (**B**) Kymographs of time-laps images corresponding to (A) along a line crossing the pollen through the germination site (left) or around the pollen grain (right). The dotted line indicates timepoint 0 of pollen tube emergence; arrowheads highlight protein accumulations at the pollen germination site. (**C**) Localisation of the ROP activity indicator *GEF12p*::CRIB4-mCit in Col-0 and *gef8-cΔ1* backgrounds. (**D**) Kymographs of time-laps images corresponding to (C) along a line crossing the pollen through the germination site (left) or around the pollen grain (right). Arrowheads highlight protein accumulations at the pollen germination site. (**E**) *LAT52p*::RGeco1 Ca^{2+} biosensor in Col-0 and *gef8-cΔ1* background. (**F**) Kymographs of time-laps images corresponding to (E) along a line crossing the pollen through the germination site. Arrowhead highlights signal increase at the pollen germination site. All scale bars represent 10 μm.

Supplemental Figures

Supplemental Figure S1: Phylogeny of all ROPGEFs of Arabidopsis thaliana and expression levels in mature pollen.

(**A**) Phylogenetic tree of the 14 ROPGEFs of *Arabidopsis thaliana* after alignment of the full-length protein sequence in Jalview, using the integrated MUSCLE alignment tool and calculation of an average distance (BLOSUM62) tree. (**B**) Presence of transcript or protein for all 14 ROPGEFs in mature pollen, according to the ATHENA – Arabidopsis THaliana ExpressioN Atlas (Mergner et al., 2020). GEFs are sorted according to the phylogenetic tree. Levels of the transcript are shown in transcripts per kilobase million (TPM) and intensity-based absolute quantifications (iBAQ) for protein levels. NA indicates that no transcript or protein was detected in this tissue.

872

Supplemental Figure S2: GEF11 and GEF13 do not accumulate at the pollen germination site.

(**A**) Protein localisation of mCit-GEF11 under its own promoter and mCit-GEF13 under control of a *GEF12* promoter fragment during pollen germination. Timepoint 0 corresponds to the beginning of pollen tube emergence, and arrowheads mark the site of pollen emergence. (**B**) Example images of mCit-GEF13 under the control of a *GEF13* promoter fragment in mature pollen grains and pollen tubes grown through a cut pistil. In neither case, any signal could be detected. All scale bars represent 10µm.

Supplemental Figure S3: Genomic structure and mutant allele information of GEF8, GEF9, and GEF12.

(**A-C**) *GEF8*, *GEF9*, and *GEF12* genomic structures with the corresponding gRNA sites (scissors) and T-DNA insertion sites (arrowhead) for *gef9-t1* (GK-717A10) and *gef12-t1* (SALK_103614). Promoter regions are shown as white boxes, UTRs in cyan, and exons in grey boxes. WT sequence for each gene and corresponding CRISPR/Cas9 deletion line is shown, and the size of CRISPR/Cas9 induced deletions is indicated. The gRNA target sequence is highlighted in colour with PAM in bold. The START and STOP codons are underlined. (**D**) *GEF9* genomic structure with T-DNA insertion sites (arrowhead) for *gef9-t1* (GK-717A10) and the location of primers used to test the mRNA presence is indicated. The table shows the expected PCR product size with the indicated primer combination for non-spliced templates (genomic) and correctly spliced templates (CDS). The gel image shows PCR products of PCRs using the indicated primer combination on cDNA from Arabidopsis flowers of Col-0 or *gef9-t1* plants.

Supplemental Figure S4: Reciprocal crosses of *GEF* mutant lines

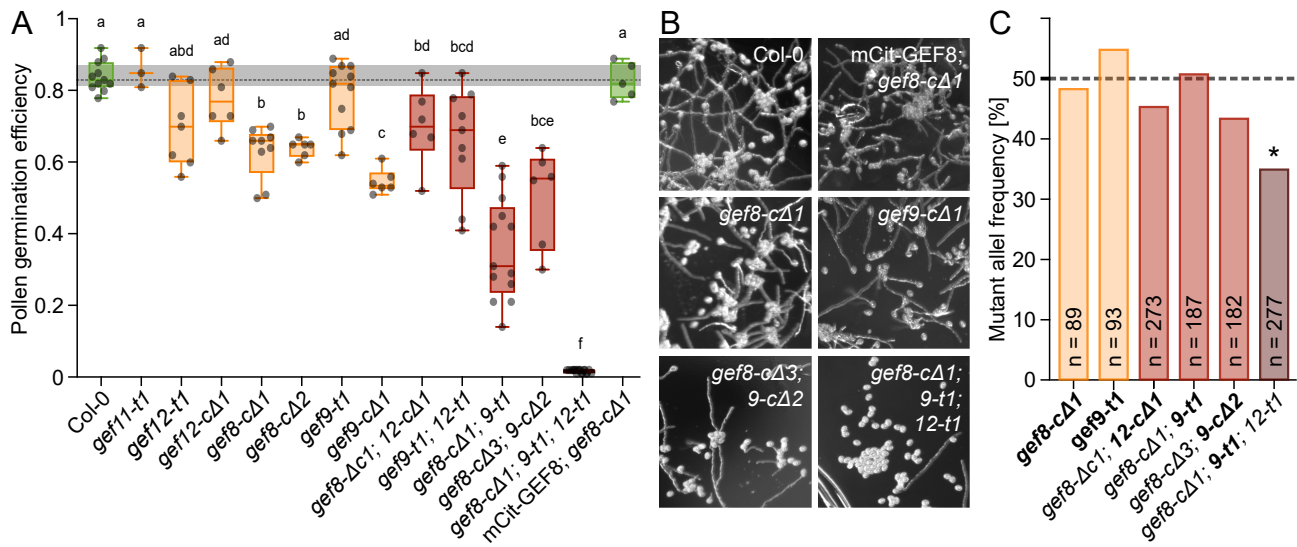Quantification of mutant allele frequency in F1 generation of reciprocal crosses with Col-0 as female and the indicated mutants as pollen donors (left) or indicated mutants as female and Col-0 as pollen donor (right). The heterozygous allele of each genotype is shown in bold. Asterisks indicate a significant difference in the allele frequency from the expected 50% according to X^2-test ($p < 0.05$)

Figure 1: GEF8 and GEF9 specifically accumulate at the pollen germination site before germination initiation
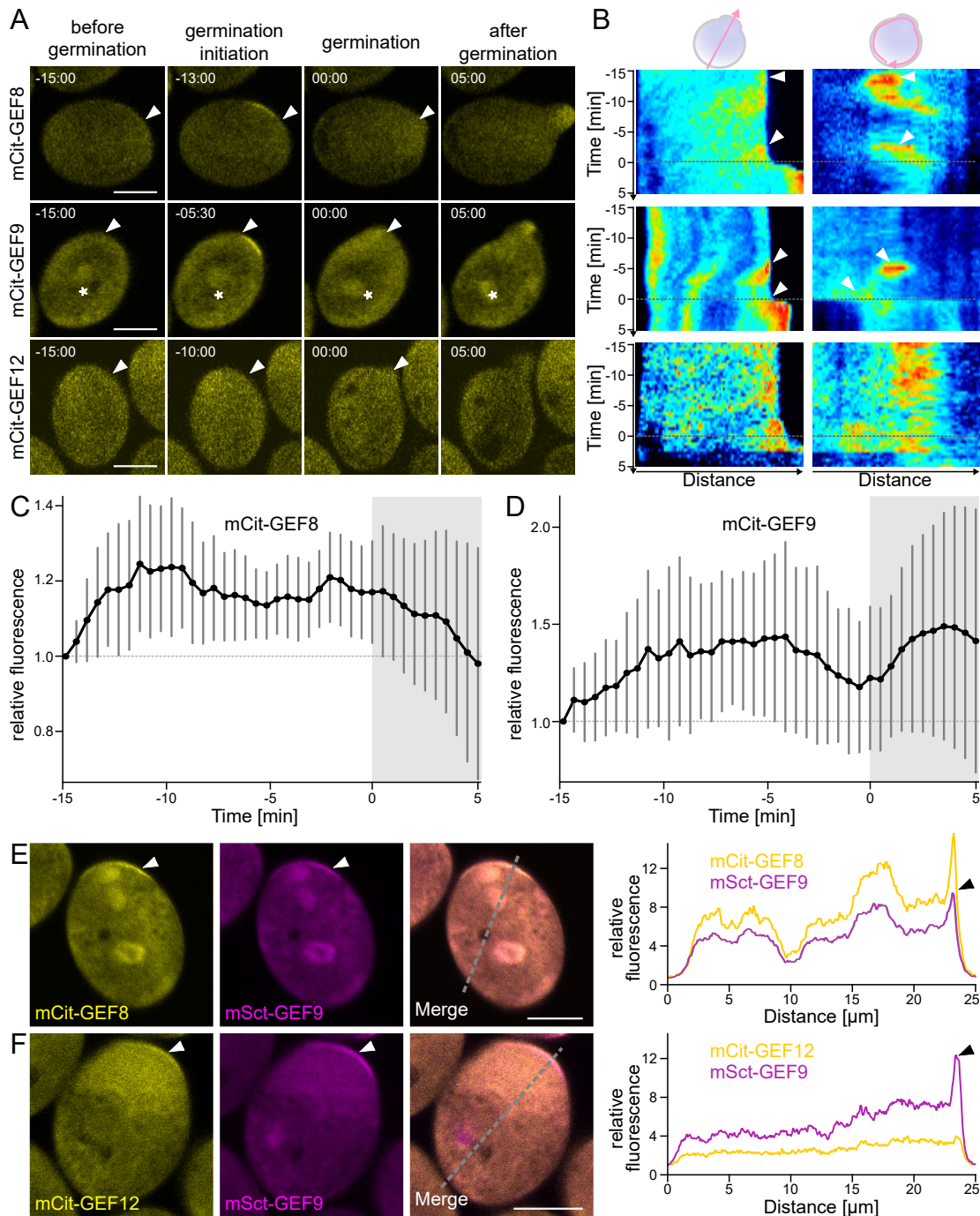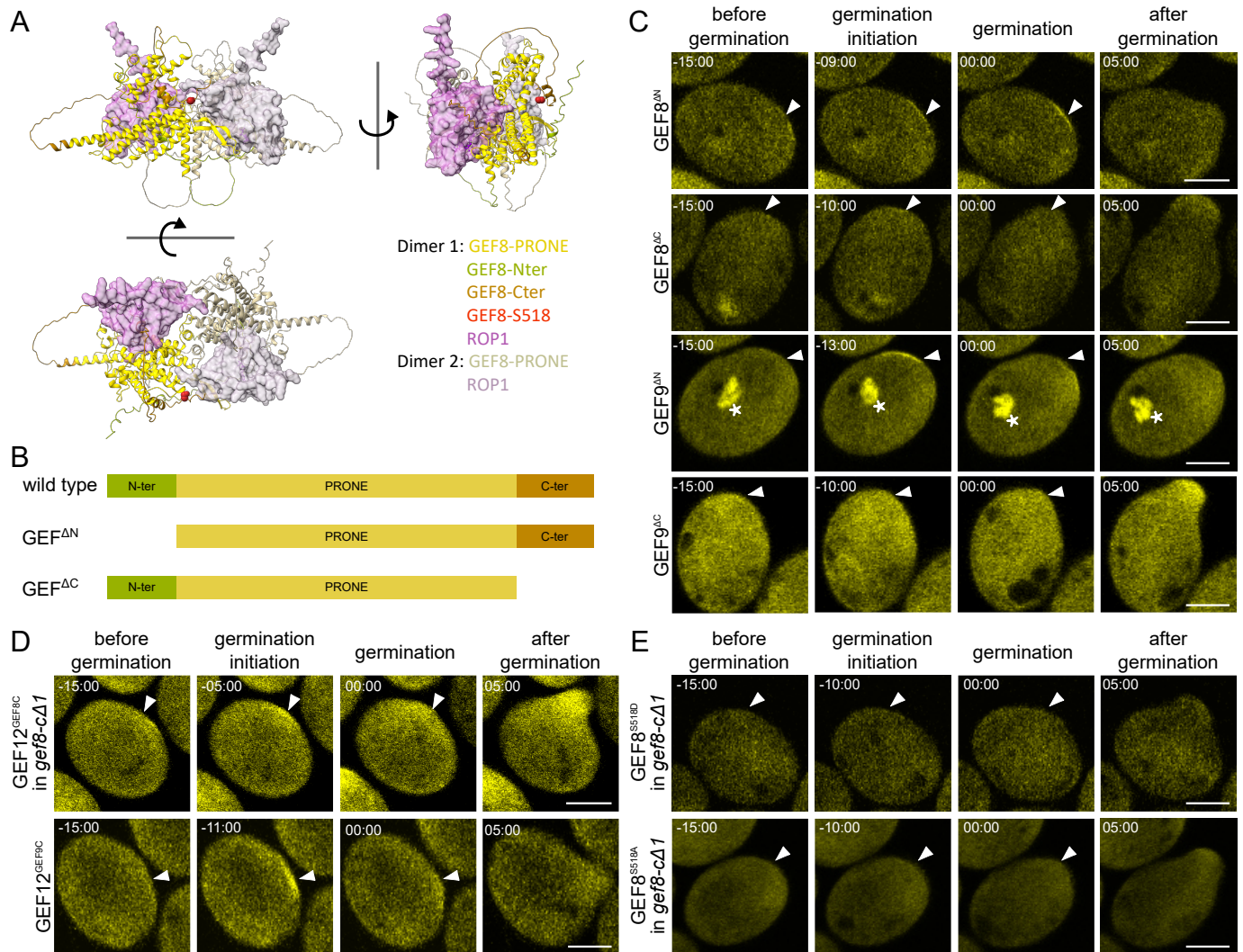

(**A**) Protein localisation of mCit-GEF8, mCit-GEF9, and mCit-GEF12 under their respective promoters during pollen germination. Timepoint 0 corresponds to the beginning of pollen tube emergence, arrowheads mark the site of pollen emergence, and asterisks mark mCit-GEF9 localisation around the sperm cells. (**B**) Kymographs of time-lapse images corresponding to (A) along a line crossing the pollen through the germination site (left) or around the pollen grain (right). The dotted line indicates Timepoint 0 of pollen tube emergence; arrowheads highlight protein accumulations at the pollen germination site. (**C & D**) Average intensity profiles of mCit-GEF8 (n=13) and mCit-GEF9 (n=12) at the pollen germination site in relation to the opposite side of the pollen grain during pollen germination. (**E & F**) Colocalization (left) and intensity profiles along a line, as indicated in the merged image, across the pollen grain through the pollen germination site (right) of mCit-GEF8 with mSct-GEF9 (E) and mCit-GEF12 with mSct-GEF9 (F) expressed under their respective promoters. All scale bars represent 10 μm.

Figure 2: GEF8, GEF9, and GEF12 are necessary for pollen germination and male fertility
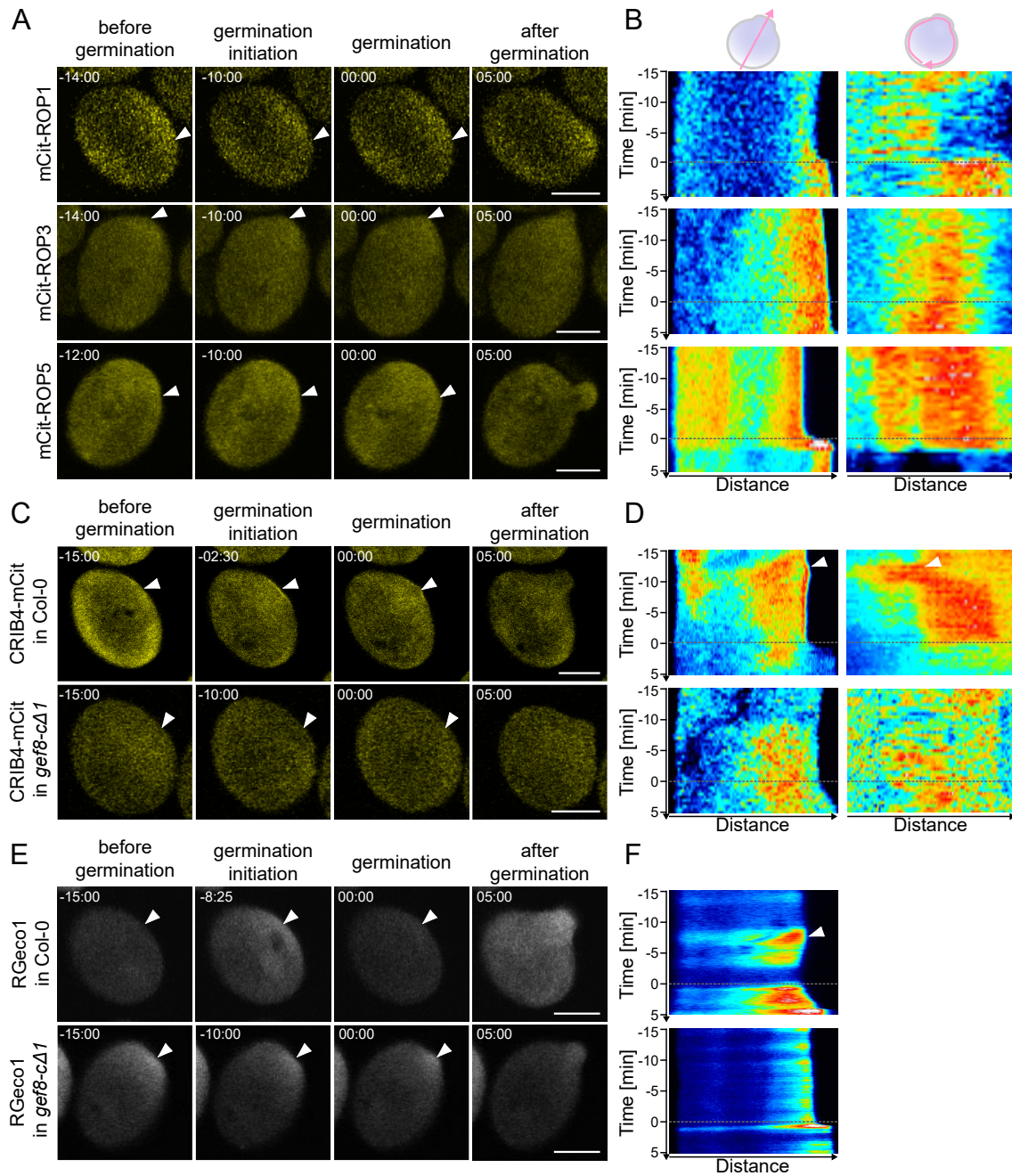

(**A**) Quantification of pollen germination efficiency of in vitro germinated pollen 4 h after imbibition on pollen germination media (PGM). Each point represents one replicate with more than 150 pollen grains. Tukey's multiple comparison test was performed by one-way ANOVA, and groups of statistically significant differences are indicated with letters (p < 0.0001). (**B**) Representative images of *in vitro* germinated pollen 4 h after imbibition on PGM. (**C**) Quantification of mutant allele frequency in F1 generation of reciprocal crosses with Col-0 as female and the indicated mutants as pollen donors. The heterozygous allele of each genotype is indicated in bold. Asterisks indicate a significant difference in the allele frequency from the expected 50% according to X2-test (p < 0.05).

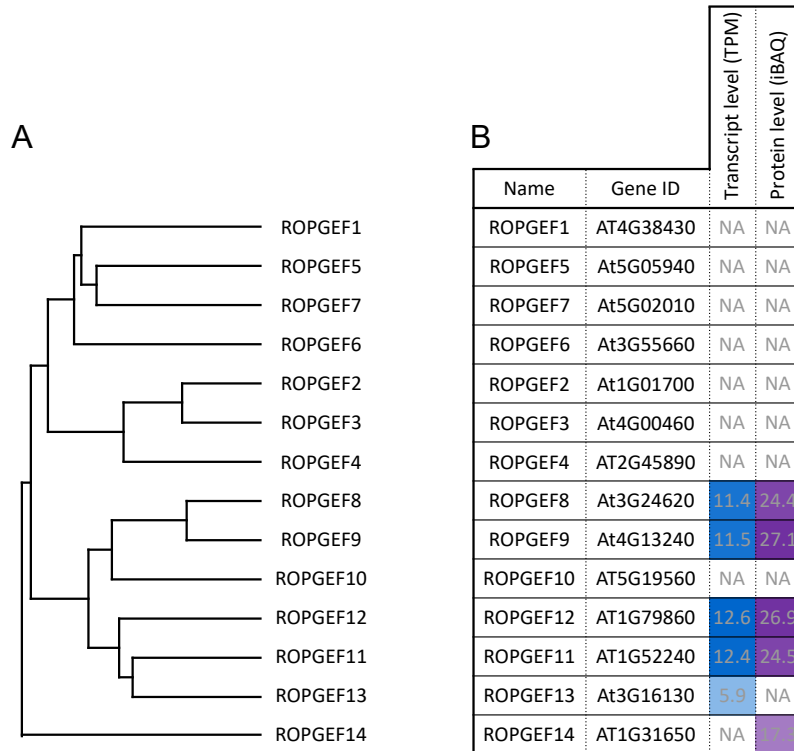**Figure 3: The C-terminus of GEF8 and GEF9 is necessary and sufficient for protein accumulation**

(**A**) AlphaFold2 protein structure prediction of full-length GEF8 and ROP1 (Rank 1, predicted separately), matched on the PRONE8-ROP4 double-dimer structure (PDB: 2NTY). Different angles are shown, and the terminal regions are indicated with different colours. (**B**) Schemes of GEF protein structure and investigated truncation constructs, with variable N and C terminal domains indicated as in (A). (**C – E**) Protein localisation of different mutant constructs under their respective promoters during pollen germination. Timepoint 0 corresponds to the beginning of pollen tube emergence, arrowheads mark the site of pollen emergence, and asterisks mark localisation around the sperm cells. (**C**) Truncation constructs mCit-GEF8$^{\Delta N}$, mCit-GEF8$^{\Delta C}$, mCit-GEF9$^{\Delta N}$, and mCit-GEF9$^{\Delta C}$ in Col-0. (**D**) Domain swap constructs of GEF12 with alternative C-terminal domain, mCit-GEF12^{GEF8C} and mCit-GEF12^{GEF9C} in Col-0. (**E**) Phosphorylation site mutations of GEF8-S518 to a phospho-mimic (mCit-GEF8^{S518D}) and phospho-dead variant (mCit-GEF8^{S518A}) variant expressed in *gef8-cΔ1*. All scale bars represent 10μm.

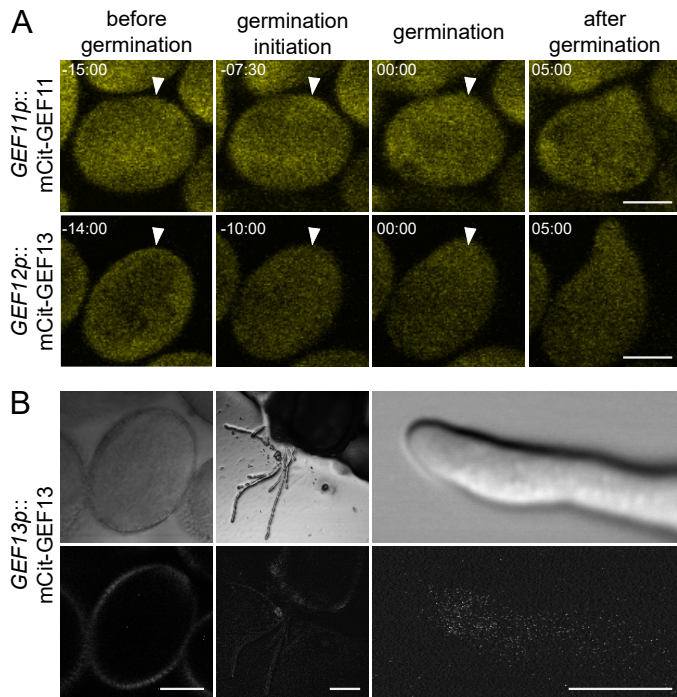## Figure 4: GEF8 is required for polar ROP activation and Ca²⁺ signalling

(**A**) Localization of mCit-ROP1, mCit-ROP3, and mCit-ROP5 under their respective promoter during pollen germination. Timepoint 0 corresponds to the beginning of pollen tube emergence, and arrowheads mark the site of pollen emergence. (**B**) Kymographs of time-laps images corresponding to (A) along a line crossing the pollen through the germination site (left) or around the pollen grain (right). The dotted line indicates timepoint 0 of pollen tube emergence; arrowheads highlight protein accumulations at the pollen germination site. (**C**) Localisation of the ROP activity indicator *GEF12p*::CRIB4-mCit in Col-0 and *gef8-cΔ1* backgrounds. (**D**) Kymographs of time-laps images corresponding to (C) along a line crossing the pollen through the germination site (left) or around the pollen grain (right). Arrowheads highlight protein accumulations at the pollen germination site. (**E**) *LAT52p*::RGeco1 Ca²⁺ biosensor in Col-0 and *gef8-cΔ1* background. (F) Kymographs of time-laps images corresponding to (E) along a line crossing the pollen through the germination site. Arrowhead highlights signal increase at the pollen germination site. All scale bars represent 10 µm.

Supplemental Figure S1 : Phylogeny of all ROPGEFs of Arabidopsis thaliana and expression levels in mature pollen

A

B

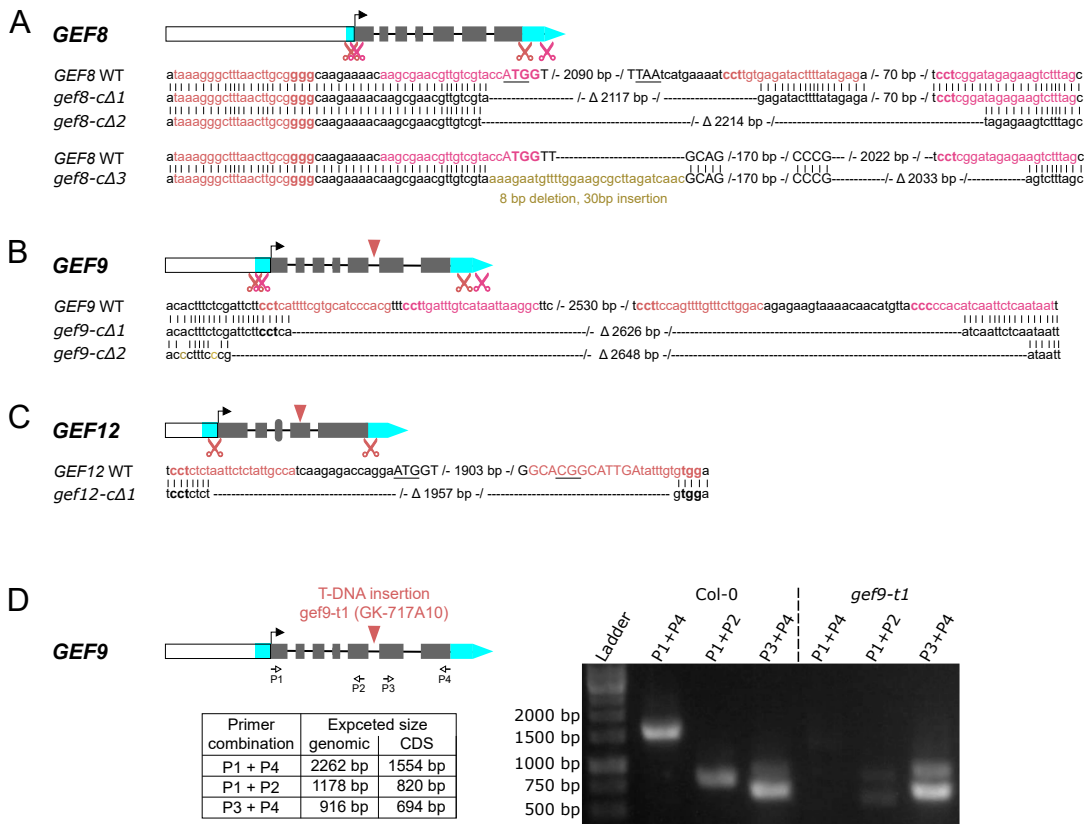| Name	Gene ID	Transcript level (TPM)	Protein level (iBAQ)
ROPGEF1	AT4G38430	NA	NA
ROPGEF5	At5G05940	NA	NA
ROPGEF7	At5G02010	NA	NA
ROPGEF6	At3G55660	NA	NA
ROPGEF2	At1G01700	NA	NA
ROPGEF3	At4G00460	NA	NA
ROPGEF4	AT2G45890	NA	NA
ROPGEF8	At3G24620	11.4	24.4
ROPGEF9	At4G13240	11.5	27.1
ROPGEF10	AT5G19560	NA	NA
ROPGEF12	AT1G79860	12.6	26.9
ROPGEF11	AT1G52240	12.4	24.5
ROPGEF13	At3G16130	5.9	NA
ROPGEF14	AT1G31650	NA	27.2

(**A**) Phylogenetic tree of the 14 ROPGEFs of Arabidopsis thaliana after alignment of the full-length protein sequence in Jalview, using the integrated MUSCLE alignment tool and calculation of an average distance (BLOSUM62) tree. (**B**) Presence of transcript or protein for all 14 ROPGEFs in mature pollen, according to the ATHENA – Arabidopsis THaliana ExpressioN Atlas (Mergner et al., 2020). GEFs are sorted according to the phylogenetic tree. Levels of the transcript are shown in transcripts per kilobase million (TPM) and intensity-based absolute quantifications (iBAQ) for protein levels. NA indicates that no transcript or protein was detected in this tissue.

Supplemental Figure S2: GEF11 and GEF13 do not accumulate at the pollen germination site.

(**A**) Protein localisation of mCit-GEF11 under its own promoter and mCit-GEF13 under control of a *GEF12* promoter fragment during pollen germination. Timepoint 0 corresponds to the beginning of pollen tube emergence, and arrowheads mark the site of pollen emergence. (**B**) Example images of mCit-GEF13 under the control of a *GEF13* promoter fragment in mature pollen grains and pollen tubes grown through a cut pistil. In neither case, any signal could be detected. All scale bars represent 10μm.

Supplemental Figure S3: Genomic structure and mutant allele information of GEF8, GEF9, and GEF12

(**A-C**) *GEF8, GEF9,* and *GEF12* genomic structures with the corresponding gRNA sites (scissors) and T-DNA insertion sites (arrowhead) for *gef9-t1* (GK-717A10) and *gef12-t1* (SALK_103614). Promoter regions are shown as white boxes, UTRs in cyan, and exons in grey boxes. WT sequence for each gene and corresponding CRISPR/Cas9 deletion line is shown, and the size of CRISPR/Cas9 induced deletions is indicated. The gRNA target sequence is highlighted in colour with PAM in bold. The START and STOP codons are underlined. (**D**) GEF9 genomic structure with T-DNA insertion sites (arrowhead) for *gef9-t1* (GK-717A10) and the location of primers used to test the mRNA presence is indicated. The table shows the expected PCR product size with the indicated primer combination for non-spliced templates (genomic) and correctly spliced templates (CDS). The gel image shows PCR products of PCRs using the indicated primer combination on cDNA from Arabidopsis flowers of Col-0 or *gef9-t1* plants.

Supplemental Figure S4: Reciprocal crosses of GEF mutant lines

Quantification of mutant allele frequency in F1 generation of reciprocal crosses with Col-0 as female and the indicated mutants as pollen donors (left) or indicated mutants as female and Col-0 as pollen donor (right). The heterozygous allele of each genotype is shown in bold. Asterisks indicate a significant difference in the allele frequency from the expected 50% according to X2-test ($p < 0.05$).

Supplemental Table S1: List of primers

Primer Name	Sqeuence	Primer ID
GEF8 Promoter with GG-Overhang A	aacaGGTCTCtACCTatggagatggatttcaaggcttga	oPDR076-F
GEF8 Promoter with GG-Overhang B	aacaGGTCTCaTGTTggtacgacaacgttcgcttg	oPDR076-R
GEF8 ORF_GG-Overhang C + ca	aacaGGTCTCaGGCTcaATGGTTGCAGCGTTGGAACG	oPDR077-F
GEF8 ORF_GG-Overhang D_STOP	aacaGGTCTCaCTGATTAATGCCTATCTTTGGGACTTCTAAAAC	oPDR077-R
GEF8 DeltaN_with ATG and STOP	aacaGGTCTCaggctcaATGGGAAAAAGATCTGAGAGACAACA	oALM16-F
	aacaGGTCTCaCTGATTAATGCCTATCTTTGGGACTTCTAAAAC	oPDR77R
GEF8 DeltaC_with ATG and STOP	aacaGGTCTCaGGCTcaATGGTTGCAGCGTTGGAACG	oPDR77F
	aacaGGTCTCaggctcaATGGGAAAAAGATCTGAGAGACAACA	oALM16-R
GEF9 Promoter with GG-Overhang A	aacaGGTCTCtACCTggggagacaataaaaagatcaaaagtatg	oPDR078-F
GEF9 Promoter with GG-Overhang B	aacaGGTCTCaTGTTggtaccaaaacctttcttttgttttcttc	oPDR078-R
GEF9 ORF_GG-Overhang C + ca	aacaGGTCTCaGGCTcaATGGTTCCATCGTTGGAACGA	oPDR079-F
GEF9 ORF_GG-Overhang D_STOP	aacaGGTCTCaCTGATCAATGCCTATCTTTAGGGCTCC	oPDR079-R
GEF9 DeltaN_with ATG and STOP	aacaGGTCTCaggctcaATGTCCCGTAGACAGGACAAGCAACAATCCGAGACG	oABM48-F
	aacaGGTCTCaCTGATCAATGCCTATCTTTAGGGCTCC	oPDR79-R
GEF9 DeltaC_with ATG and STOP	aacaGGTCTCaGGCTcaATGGTTCCATCGTTGGAACGA	oPDR79-F
	aacaGGTCTCaCTGATTCACCTGTGCATTGCTTCCGGGCTAA	oABM49-R
GEF12 Promoter with GG-Overhang A	aacaGGTCTCtACCTatctccttttctctgtttttttttttttatttttcttc	oPD0139-fwd
GE12 Promoter with GG-Overhang B	aacaGGTCTCaTGTTtcctggtcccttgatggcaatagag	oPD0139-rev
GEF12 Part A with GG-Overhang C	aacaGGTCTCtGGCTATGGTTCGTGCTTCGGAACA	oPD0140A-fwd
GEF12 Part A for BsaI-Site mutation	aacaGGTCTCGATCCGGTGGCAGCCTCATCTAAACC**a**GTCTCGAC	oPD0140A-rev
GEF12 Part B	aacaGGTCTCCGGATCCCATGACGCTGAA	oPD0140B-fwd
GEF12 Part B	aacaGGTCTCTCTCGCTTCTCCAGACTTACTC	oPD0140B-rev
GEF12 Part C for BsaI-Site mutation	aacaGGTCTCGCGAGAGGTCTTCGAAGAGCGAGCTGA**a**ACCATTTTG	oPD0140C-fwd
GEF12 Part C with GG-Overhang D	aacaGGTCTCtCTGATCAATGCCGTGCCGTTGG	oPD0140C-rev
GEF12Nter-PRONE	aacaGGTCTCtGGCTcaATGGTTCGTGCTTCGGAACA	oPDM22F
	aacaGGTCTCtGCTTGTTCCCCGCTCGATCTGC	oABM71-RA
GEF8 Cter	aacaGGTCTCaAAGCAAACTTTATTGGCTGAAGA	oABM071-R-B
	aacaGGTCTCaCTGATTAATGCCTATCTTTGGGACTTCTAAAAC	oPDR77R
GEF9 Cter	aacaGGTCTCcaAGCAATGCACAGGTGAAGAA	oABM072-R-B
	aacaGGTCTCaCTGATCAATGCCTATCTTTAGGGCTCC	oABM79R

CRISPR GEF8 deletion gef8-c1	aacaGGTCTCgATTGagcgaacgttgtcgtaccaGTTTTAGAGCTAGAAATAGC	oABM01-F
	aacaGGTCTCgAAACtgtgagatactttatagacAATCTCTTAGTCGACTCTAC	oABM01-R
CRISPR GEF8 Pair 1 Stuttmann Cloning	acaGAAGACtgATTGtaaagggctttaacttgcgGTTTCAGAGCTATGCTGGAAACA	oABM73-F
	acaGAAGACtgAAACcggatagagaagtctttagCAATCACTACTTCGACTCTAGCTG	oABM73-R
CRISPR GEF8 Pair 2 Stuttmann Cloning	acaGAAGACtgATTGagcgaacgttgtcgtaccaGTTTCAGAGCTATGCTGGAAACA	oABM74-F
	acaGAAGACtgAAACtgtgagatacttttatagaCAATCACTACTTCGACTCTAGCTG	oABM74-R
CRISPR GEF9 Pair 1 Stuttmann Cloning	acaGAAGACtgATTGcgtgggatgcacgaaaatgGTTTCAGAGCTATGCTGGAAACA	oABM75-F
	acaGAAGACtgAAACtccagttttgtttcttggacAATCACTACTTCGACTCTAGCTG	oABM75-R
CRISPR GEF9 Pair 2 Stuttmann Cloning	acaGAAGACtgATTgccttaattatgacaaatcaGTTTCAGAGCTATGCTGGAAACA	oABM76-F
	acaGAAGACtgAAACcacatcaattctcaataatCAATCACTACTTCGACTCTAGCTG	oABM76-R
gef8-c1 genotyping	agtccttaaaatcgaaaacaaacgt	oABM18-LP
	ctttggagtttggaccatacgc	oABM18-RP
	GGACATGTCGACAGAGCACA	oABM18-Int
gef9-c2 genotyping	acggaagcacaaaccactga	oABM19-LP
	acgacttcatgtgcacacac	oABM19-RP
	tgcctttgcagtcgagtgtt	oABM19-Int
gef9-t1 genotyping	GGCACTATCAAATGCCATCAC	oFA009_LP
	TCTTTTCCATATAACGATTGAGG	oFA009_RP
gef11-t1 genotyping	TCAGAGAGAGGTCAAAATTGAGG	oPD0168-LP
	TACCTGCGAGATTGGTAATGG	oPD0168-RP
gef12-t1 genotyping	AGGAGTATCCTCTGCTCTCGC	oPDM008-LP
	ATGATTGATGCCTCGATTCTG	oPDM008-RP

Supplemental Table S2: List of cloned expression vectors

		Promoter	N-terminal Tag	ORF / CDS	C-terminal Tag	Terminator	Plant selection	Expression Vector	Bacterial selection marker	Plasmid ID
		Module A	Module B	Module C	Module D	Module E	Module F	Module Z		
Green Gate Vector Cloning	mCit-GEF8	GEF8-Promoter	mCitrine w/ Linker	GEF8-ORF	Decoy	HSP18.2	Basta	pGGZ003	Spec/Strep	pPDR124
	mCit-GEF9	GEF9-Promoter	mCitrine w/ Linker	GEF9-ORF	Decoy	HSP18.2	Basta	pGGZ003	Spec/Strep	pPDR125
	mCit-GEF12	GEF12-Promoter	mCitrine w/ Linker	GEF12-ORF	Decoy	HSP18.2	Basta	pGGZ003	Spec/Strep	pPD0304
	mSct-GEF8	GEF8-Promoter	mScarlet w/ Linker	GEF8-ORF	Decoy	HSP18.2	Hygromycine	pGGX000	Kanamycince	pABM04
	mSct-GEF9	GEF9-Promoter	mScarlet w/ Linker	GEF9-ORF	Decoy	HSP18.2	Hygromycine	pGGX000	Kanamycince	pABM05
	mSct-GEF12	GEF12-Promoter	mScarlet w/ Linker	GEF12-ORF	Decoy	HSP18.2	Hygromycine	pGGX000	Kanamycince	pABM06
	mCit-GEF8ΔN	GEF8-Promoter	mCitrine w/ Linker	GEF8-ORFΔN	Decoy	HSP18.2	Basta	pGGYR0	Spec/Strep	pABM93
	mCit-GEF8ΔC	GEF8-Promoter	mCitrine w/ Linker	GEF8-ORFΔC	Decoy	HSP18.2	Basta	pGGYR0	Spec/Strep	pABM94
	mCit-GEF9ΔN	GEF9-Promoter	mCitrine w/ Linker	GEF9-ORFΔN	Decoy	HSP18.2	Basta	pGGYR0	Spec/Strep	pABM76
	mCit-GEF9ΔC	GEF9-Promoter	mCitrine w/ Linker	GEF9-ORFΔC	Decoy	HSP18.2	Basta	pGGYR0	Spec/Strep	pABM77
	mCit-GEF12GEF8Cter	GEF12-Promoter	mCitrine w/ Linker	GEF12-ORF+ GEF8Cter	Decoy	HSP18.2	Basta	pGGYR0	Spec/Strep	pABM83
	mCit-GEF12GEF8Cter	GEF12-Promoter	mCitrine w/ Linker	GEF12-ORF+ GEF9Cter	Decoy	HSP18.2	Basta	pGGYR0	Spec/Strep	pABM84
	Gef12p::RIC4-CRIB:mCit	GEF12-Promoter	Omega element for enhaced translation	RIC4-CRIB	mCitrine w/ Linker	HSP18.2	Basta	pGGYR0	Spec/Strep	pPDM117
	Lat52::RGeco1	Lat52 promoter	Decoy	RGeco1	Decoy	HSP18.4	Hygromycine	pGGX000	Kanamycince	pFA18
	GEF8 GEF9 CRISPR	GEF8 gRNAs- pair 1	GEF8 gRNAs- pair 2	GEF9 gRNAs- pair 1	GEF9 gRNAs- pair 2	-	-	pDGE347	Spec/Strep	pABM90